Drop Response Using a Compact Wake Spreading Model

// Texas A&M University.

SHIP RESPONSE USING A COMPACT WAVE SPECTRUM MODEL

A Thesis

by

LARRY DONALD LINN

Submitted to the Graduate College of
Texas A&M University
in partial fulfillment of the requirements for the degree of

MASTER OF SCIENCE

May 1985

Major Subject: Ocean Engineering

SHIP RESPONSE USING A COMPACT WAVE SPECTRUM MODEL

A Thesis

by

LARRY DONALD LINN

Approved as to style and content by:

ABSTRACT

Ship Response Using a Compact Wave Spectrum Model. (May 1985)

Larry Donald Linn, B.S. of Naval Architecture,

United States Naval Academy

Chairman of Advisory Committee: Dr. John M. Niedzwecki

A multivariate statistical technique, known as principal component analysis, is used to compact large data bases of theoretical and real spectral information. Statistical properties of the various data bases are examined in their original and compacted forms. Sensitivity to spectral width and spectral shape is also studied. The original and compacted wave data bases are then used to excite sets of ship response amplitude operator's (RAO's). The resulting response spectra are examined both statistically and for any sensitivities to spectral characteristics. It is found that principal component analysis accurately compacts wave data bases and ship response spectra of a wide range of spectral shape. The statistical characteristics of the reconstructed spectra are also found to compare extremely well with the statistics of the original data set.

ACKNOWLEDGEMENT

The author wishes to express his sincere appreciation to his family, near and far, for their unfailing support and encouragement throughout graduate school and the completion of this report.

The author is also indebted to Mr. F. W. Boye of Shell Development Company for making available field data for use in this study and to Dr. Roger Compton of the United States Naval Academy, Naval Architecture Department for making available ship response data also used in this study.

Finally, my sincere apppreciation goes to Dr. John M. Niedzwecki, committee chairman and advisor, for his guidance, support and encourgement throughout the research and preparation of this report as well as the completion of my graduate studies.

TABLE OF CONTENTS

LIST OF TABLES

LIST OF FIGURES

CHAPTER I

INTRODUCTION

The random behavior of the ocean environment poses a major problem to the naval architect in the design of a ship or vessel. The proper vessel design is essential for the ship to meet planned objectives and to fulfill its mission. A review of historical shipbuilding activities clearly shows that ships and vessels have become more and more mission specific. Current examples of this include fast passenger vessels, merchant cargo ships and a variety of specialized naval ships. Each individual vessel or class of ship must, therefore, be designed with its intended mission in mind and a set list of design criteria established and agreed upon between the designer and eventual user. It then becomes the naval architect's responsibility to insure that the ship will not only be able to ride out the roughest storms designed for but that the ship can proceed in its mission under these severe conditions with a minimum of delay. The eventual "sea-going performance" and its evaluation as good or bad can be based on certain desirable features of the specific ship. Some possible features could include low accelerations, minimum slamming, minimum deck wetness and ease of steering. Each in itself should not be used as an absolute measure of the ship's performance. For example, the mission of a merchant ship is to deliver its cargo and

---

The citations on the following pages follow the style of the "Journal of Ship Research," Society of Naval Architects and Marine Engineers.

passengers, at its destination, safely and promptly, regardless of the encountered ocean environment. It can then be said that for merchant ships, in general, "the ultimate criterion of good seagoing performance is (the) ability to maintain speed in rough seas [1]." The naval architect will study the situation and decide upon numerous things from a general hull form, total power requirements, fuel consumption, overall ship dimensions, basic proportions, natural periods of oscillation, and so forth. He will also be extremely concerned with the ship's motion in waves, more specifically, how this ship will respond to the ocean environment in which it must operate. To do this he must know something about the medium in which it will function, the ocean.

St. Denis and Pierson stated that the most characteristic feature of the ocean is that the surface is irregular and never repeats itself [2]. Even though the sea is irregular there are periods of time when a large section of open water might maintain a particular steady appearance. This observation suggests the possibility of describing the seaway by statistical characteristics including significant wave height and period. Later research has indicated that if these statistical features are applied to an equivalent regular series of waves, for model testing, it could lead to a gross estimate of the actual forces and motions that might be anticipated or experienced [3]. Again realizing that the ocean waves are irregular and that modern day towing tanks are capable of producing an irregular wave train it is important to understand why model testing with an irregular wave train is not commonplace. In order to assure that

statistically maximum wave heights are experienced a very long run is necessary. The resulting long wave record must be then analyzed to establish the values achieved, corresponding frequencies, etc. If response characteristics for the model with headway are desired the amount of usable data is severely restricted by the length of the available tank. Overall, direct irregular sea tests are considered cumbersome, labor intensive and susceptible to error. On occasion, some tests are run but more as a check of predetermined results or to approximate some general realistic behavior pattern.

In a further attempt to better characterize the ocean environment, oceanographers have found that by using general harmonic analysis techniques it is possible to represent the sea surface by the sum of an infinite number of regular, small amplitude, sine waves. Each independent wave will vary in period, length, amplitude, direction. A sample illustration on how a small number of regular waves of different heights and lengths can result in an irregular sea is shown in Fig. 1. Spectral theory suggests that although the seaway is irregular and made up of these numerous, small amplitude waves the total energy of the sea within a given area must remain at a constant for a duration of time. The total energy of the sea must then be comprised of the sum of energies of all the small, regular waves (component waves). It is known that for each square foot of water surface the energy of a simple sinusoidal wave is

$$\rho g H^2/8 \quad .$$

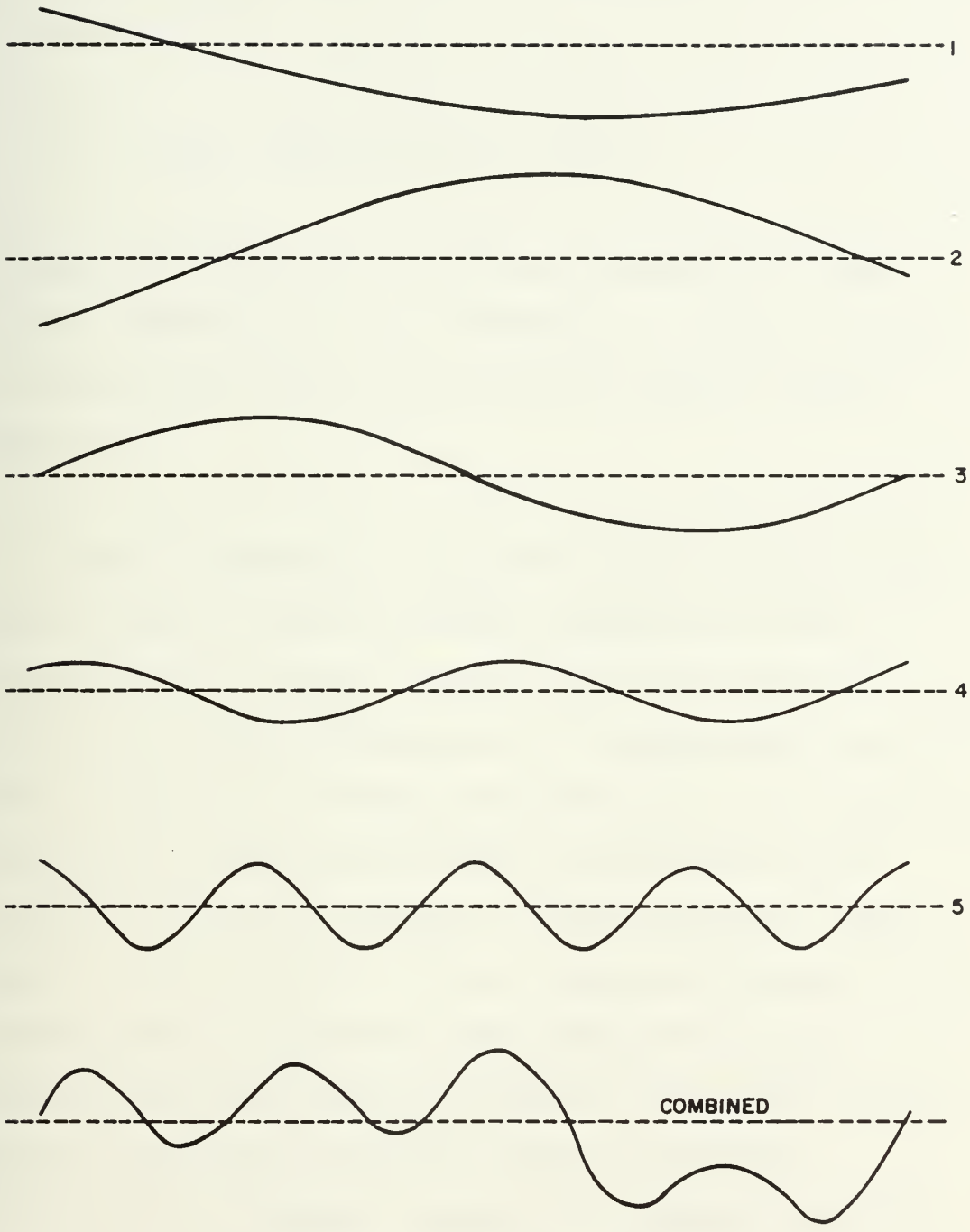

Fig. 1. Wave pattern combining five regular waves [3].

Therefore, the energy contained within each square foot of seaway would then be proportional to the sum of the squares of the heights of the component waves

$$\text{Energy} = (\rho g/8)(h_1^2 + h_2^2 + h_3^2 + \ldots .) \quad .$$

Any seaway may now be characterized by a representative "energy spectrum" indicating the relative importance, or amount of energy, in the component waves combining to produce the observed irregular pattern [1].

An important aspect in using spectral theory to represent the ocean environment is that it provides a complete statistical characterization of the sea. The next step in determining and evaluating the response characteristics of a design ship rests in the ability to relate the wave energy spectrum to actual ship responses. Through detailed research of the ocean and based upon laws of statistics, the surface of the sea is assumed to follow a normal "Gaussian" type distribution. Study of actual ship motions within an ocean environment indicates that these motions have the same properties as do wave records. The essential idea is that the ship motions are also a Gaussian process and can be completely characterized by a "response" spectrum. This indicates that the response of a ship in a confused sea is steady-state and not a series of transient processes. As both wave record and corresponding ship motions exhibit similar properties each spectrum may be related to the other by characteristic functions of the vessel known as Response

Amplitude Operator's (RAO's). RAO's are defined as functions which yield the amplitude of the oscillatory response of the ship on or about one of the principal axes when in a regular seaway of unit amplitude [2]. In simpler terms, it is the unit response of the motion or force of a body per foot of wave height. The capability presently exists to determine the ship RAO's either by theoretical means or by a superposition of vessel/model responses to wave components making up the seaway. In each method there are certain inherent difficulties or limitations involved, however, these will not be addressed within this text. Since the response functions can be determined in a controlled environment the resulting experimental RAO's are found to be accurate to the precision of the monitoring and measuring devices. An example of a pitch and heave RAO is found in Fig. 2. The concept of a RAO is a valuable tool to predict the performance of a new vessel design, or of modified designs, in any desired sea condition, "so long as the sea condition can be specified by means of a suitable spectrum [1]." This is the challenge.

Individual wave spectra can have a variety of shapes. The shape depends on numerous factors including local wind velocity, wind duration, fetch, and affects of localized storm systems from which swell may travel. Two of the most important parameters are the duration and velocity of the local wind. As wind forces generate surface waves the resultant sea spectrum grows in energy beginning at the high frequency end and, provided the wind continues to blow, slowly shifts to the lower frequencies. If the wind maintains for a

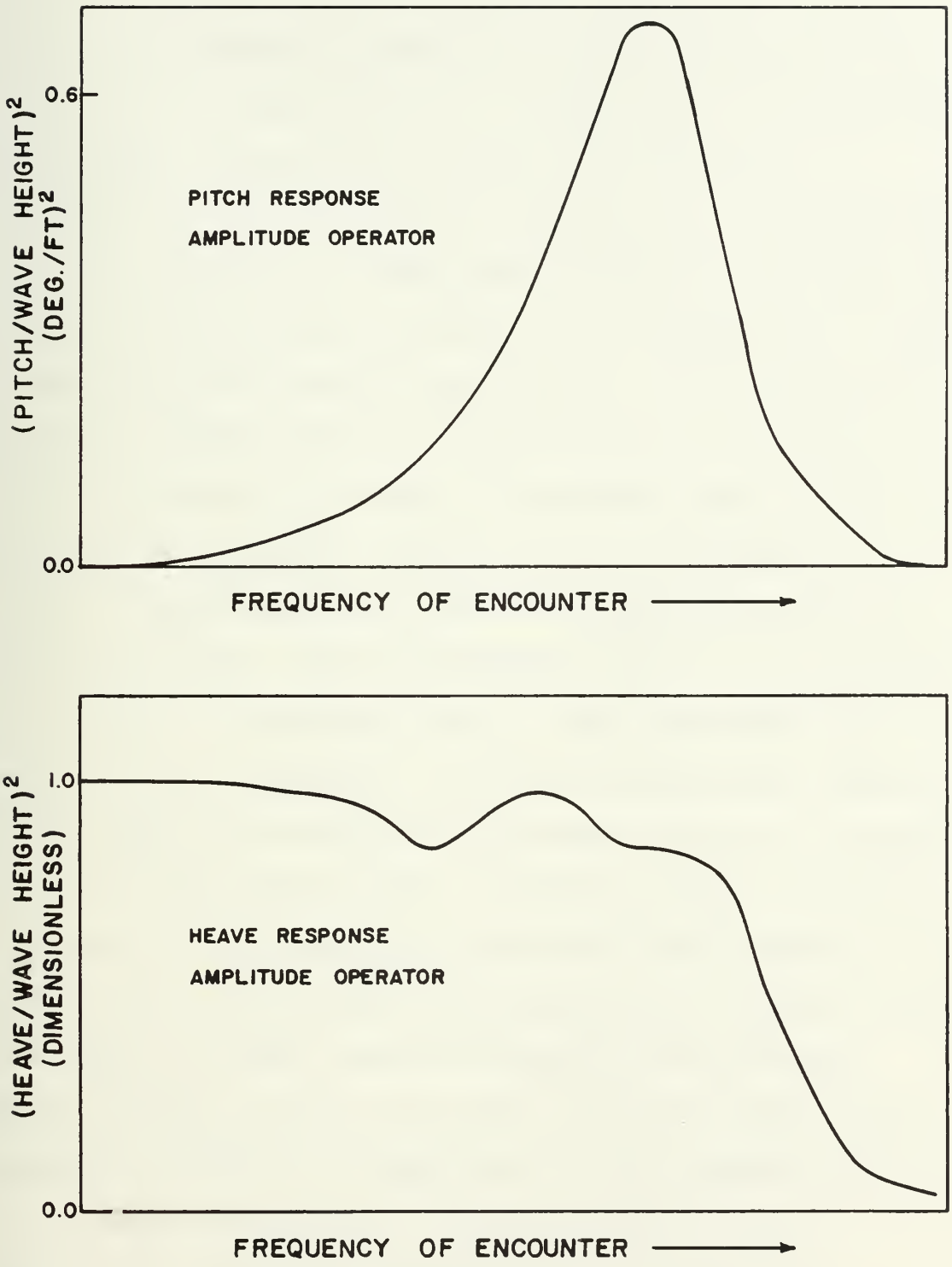

Fig. 2. Pitch and heave RAO's for a 500 foot ship (RAO set 1).

sufficient duration the sea system becomes stable and no further effect will be produced no matter how long the wind continues to blow. This condition is known as the "fully developed sea". There have been many attempts to artificially "reproduce" the design ocean environments through the use of wave spectrum models. Major problems associated with the use of these spectrum models are that they are all site specific and usually describe only fully developed seas. Efforts to generalize various popular models have led to the introduction of additional parameters which are intended to account for the local variations observed in real data. The available spectrum models fall into two basic categories. Formulas which use the first, or "classic," approach use wind speed as the independent variable to define the spectrum. The Pierson-Moskowitz Spectrum is an example of this type and is illustrated in Fig. 3. Later models define the spectrum using as independent variables the characteristic properties of the seaway such as significant wave height and period. An example is the Ochi-Hubble Spectrum that is generated using the significant wave height. Fig. 4 illustrates a sample Ochi-Hubble spectrum. An example of a spectrum obtained from real wave data is shown in Fig. 5. This example was chosen from the real data base being analyzed. Whatever approach is chosen, the values selected for these varying parameters are left to the discretion of the ship designer based on his knowledge and experience. As a result, there is a real possibility of inaccurately representing the encountered sea conditions and subsequently making wrong design decisions.

An energy spectrum may also be produced using actual wave data

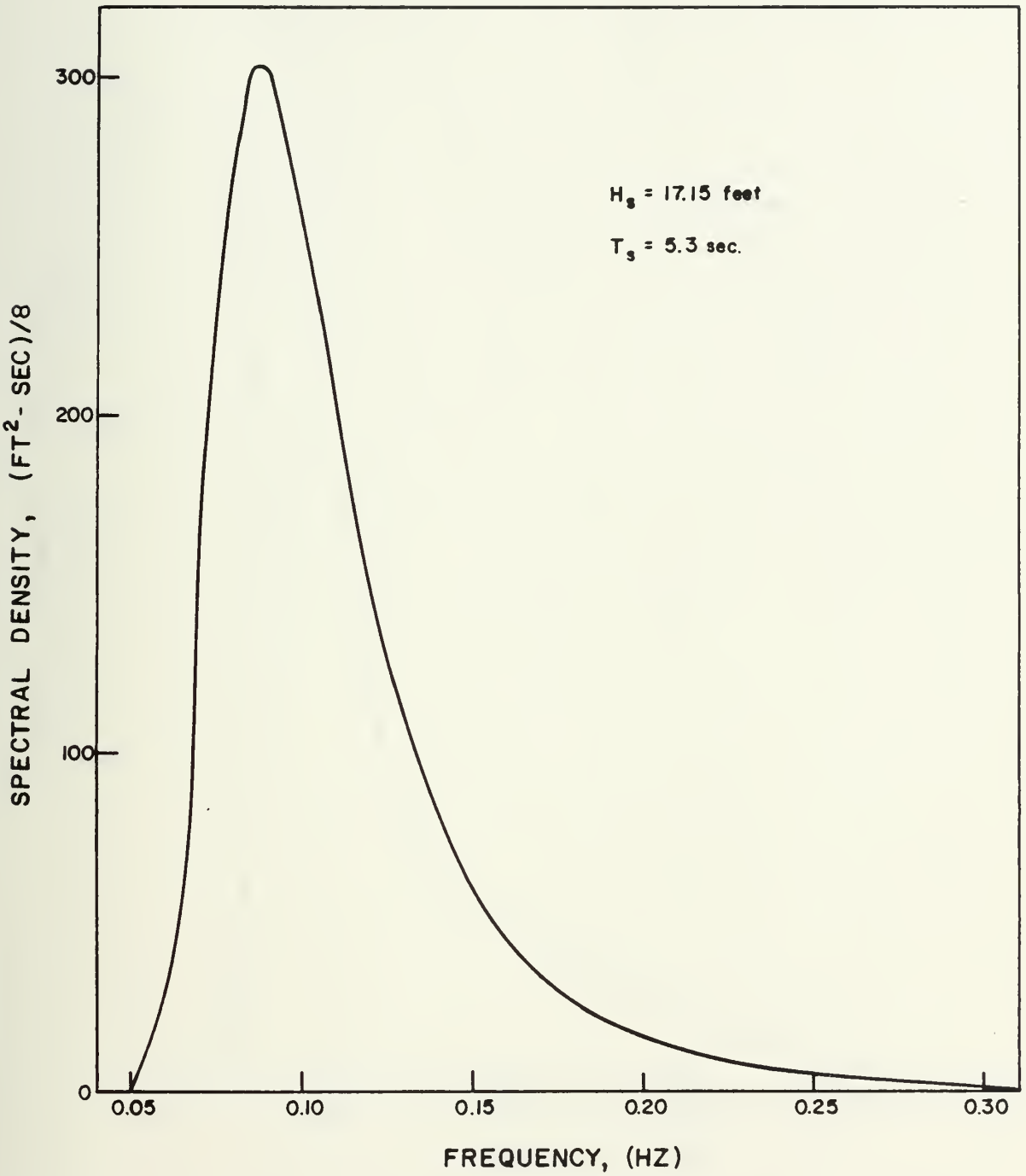

Fig. 3. Sample Pierson-Moskowitz wave spectrum.

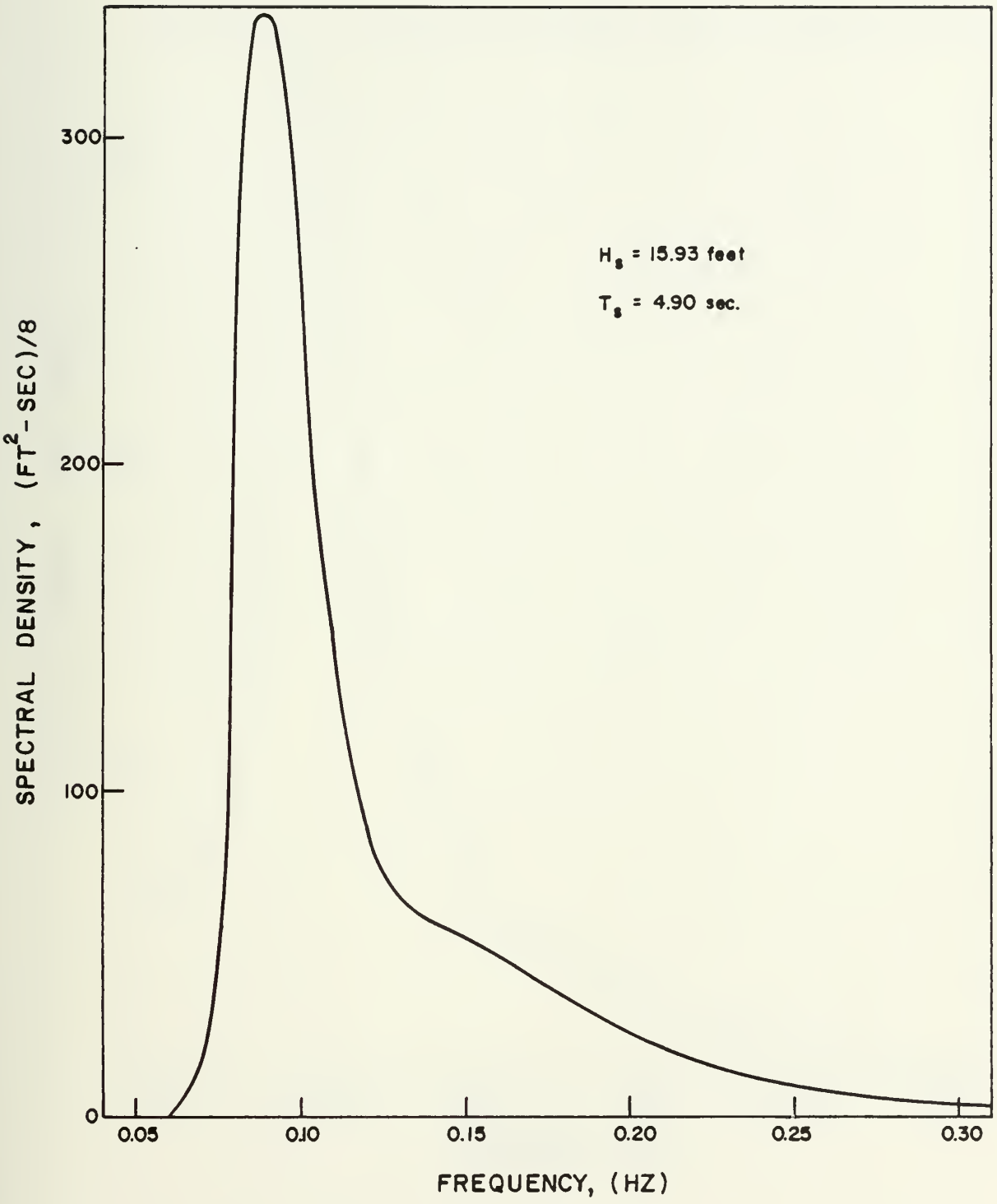

Fig. 4. Sample Ochi-Hubble wave spectrum.

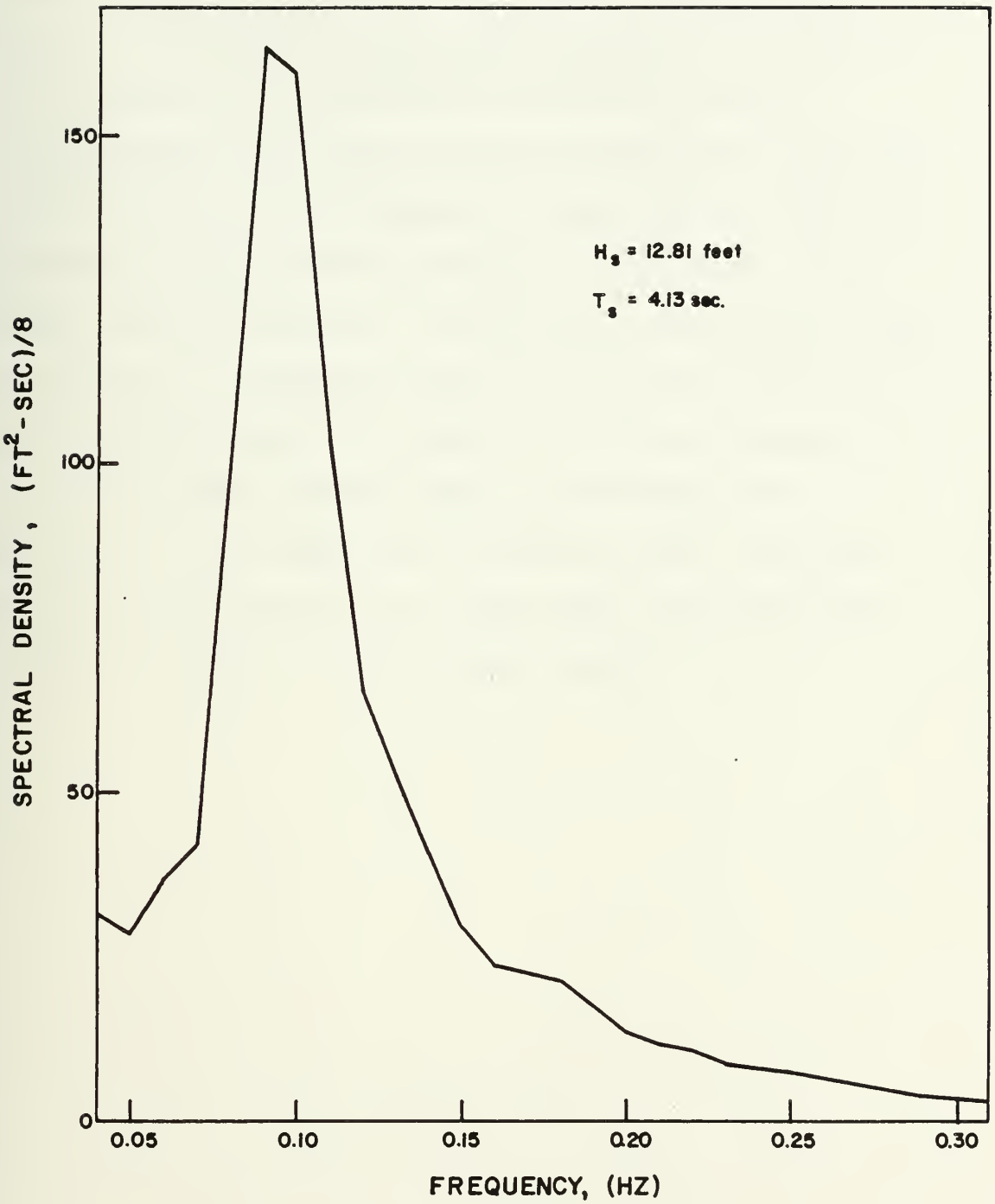

Fig. 5. Sample real data wave spectrum.

and creating a spectrum by applying generalized harmonic analysis techniques. To accurately represent the local ocean environment by use of this method requires significant amounts of wave data. Sophisticated monitoring systems have been developed which are capable of providing large quantities of data in a short period of time. With these systems an ever increasing data base of information is made available to the ship designer. The difficulties now facing the naval architect are: 1.) condensing the data into an usable form, and, 2.) using this new data base in the design and evaluation processes. It is clear that engineering design procedures must become more probabilistic in their nature and, if information from large data bases is to be used properly, more research must be focused on the development of probabilistic ship design procedures.

CHAPTER II

LITERATURE REVIEW

Considerable effort has been expended over the decades in an effort to establish a universal wave spectrum model with which to use as a basis for design evaluation and research. Individual models have ranged from those containing a single, independent parameter to those including numerous independent variables. Attention has also focused upon including directionality into the spectrum. In each instance, the validity of the resulting model has remained in doubt causing attention now to be focused on preserving inherent characteristics of site specific data and, hence, foregoing the use of overly simplistic parametric models. To accurately represent the seaway without losing essential statistical values a large data base is required. In dealing with the ocean environment the availability of large quantities of data has improved because of increasing sophistication of monitoring devices deployed and the advancement of hindcasting techniques. The problem now exists of how to condense this data base into something usable. In the past, multivariate statistical techniques have been used to study sets of random variables, in particular, the relationship between them as suggested by the data. An advanced multivariate statistical technique, known as principal component analysis, is a promising methodology that has been used by engineers and scientists desiring to investigate wide ranging problems involving large quantities of time series and spectral data [4].

Principal component analysis is a procedure similar to standard eigen analysis methods and allows for an orthogonal transformation of the entire data base. In this way a set of empirical eigenfunctions, which best fit the data base, are found. The orthogonality of the eigenvectors and associated coefficients insure independent predictors and represent a percentage of the total value or total variance of the data set. The eigenvector associated with the largest eigenvalue represents the greatest portion of the total value with each succeeding eigenfunction representing proportionally less. Experience has shown that a comparatively small number of eigenfunctions are required to represent extensive banks of data. Therefore, the remaining functions, which contribute little to the total representation, can be disregarded. The next step, and probably the most difficult, is to find a physical interpretation for each of the remaining significant eigenfunctions, or principal components. Research in several different fields of study have been able to identify principal components and to correspond these, with reasonable accuracy, to observed natural occurrences.

Although the basic methodologies used in each of the reviewed studies are similar, some variations in the analysis procedures can be identified. These differences are attributed to the nature of the data bases being analyzed and the type of natural process being investigated. The data is structured into a symmetric matrix from which the eigenfunctions are then derived. The basic nature of the original data base is maintained within the symmetric matrix and is

reflected in the resulting output. A summary of various types of data input that result in the first eigenfunction resembling an observed natural process is shown in Table 1.

Table 1. Summary of input/output structuring.

Type of Structured Data Base	Type of Symmetric Matrix	First Eigenfunction Highest Resemblance to:
Actual Values	Cross-Product Matrix	Observed Fields
Departure from Means	Covariance Matrix	Departure Fields
Normalized Departure from Means	Correlation Matrix	Normalized Departure Fields

Investigations [5] and [6], by Hashimoto and Uda, studied coastal beach profile changes using empirical eigenfunction analysis. In each study the data received was analyzed as a time series to detail coastal sand transport caused by wave action and offshore currents. The method of data collection utilized in [5] necessitated that eigenfunctions be derived from a symmetric correlation matrix after subtracting out the temporal mean of the beach profile. The symmetric correlation matrix was computed from variables representing normalized departures from the mean. The use of normalized variables assured that each variable at each point in the field was of equal importance in determining the form of the representation. It follows that the first eigenfunction will have the highest resemblance to the normalized departure field. By comparing the eigen- and weighting

function changes over time the authors were able to identify accretion/erosion processes and to correlate the first and second eigenfunctions to shifts in longshore and onshore-offshore sand transport, respectively. The rate of longshore transport was mainly dependent on wave height and direction while the onshore-offshore transport relied mainly on wave height changes.

Uda and Hashimoto [6] extended this approach by applying it to sand transport and beach profile changes near a breakwater. As in their previous work, the beach profile data was analyzed at certain longshore intervals to obtain the spatial characteristics of the profiles. The eigenfunctions were determined from a symmetric matrix of normalized measured values without subtracting a mean value. As mentioned previously, using data based on beach profile variations provides for an analysis of characteristic beach changes instead of the beach profile itself. The symmetric matrix was able to be reduced to three significant eigenfunctions each exhibiting only a slight dependence with time. The time variations of observed beach profiles were accounted for by time dependent adjustments in the weighting functions. The product of the eigenvectors with their respective weighting functions led to the conclusion that the first eigenfunction corresonded to the mean beach profile, the second to profile changes caused by longshore sand transport and the third eigenfunction to changes due to the influence of the nearby breakwater.

A study of coastal beach profile changes normal to the shoreline was conducted by Winant et al. [7]. Previous research had identified

that the sand level elevations for the beaches being monitored could vary as much as several meters between the summer and winter months. More specifically, a net sand transport existed towards the beach during the spring and summer months with the process reversed through the fall and winter seasons. The onshore transport process eventually resulted in a steep beach face and an adjacent high berm. This summer berm was subsequently eroded by waves generated from winter storms. The offshore sediment motion accounted for an accumulation of sediment offshore beyond the surf zone. This newly created beach feature is commonly referred to as the winter bar. This study, [7], primarily concerned itself with the three basic beach features that account for the majority of changes in beach configuration and are most useful in describing variations.

Data collected consisted of beach elevations generated as a linear combination of functions of distance normal to the beach and as a function of time. The data base exhibited a slight trend in time so that the eigen analysis was performed on the correlation matrix. The eigenfunction associated with the largest eigenvalue, and therefore the greatest percentage of value, was found to reflect the mean beach elevation. This is referred to as the "mean beach function". The second eigenvalue comprised approximately forty (40) percent of the variance of data from the mean beach function. The corresponding function is called the "bar-berm function". In summer months the summation of the mean beach and bar-berm functions account for the onshore sand transport and the development of the summer berm. The summation of these two functions during the winter months account for

the diminishing of the summer berm and the reforming of the winter bar by offshore sand transport. As would be expected, this second function shows a very strong yearly time dependence. The third function identified accounted for an additional thirty (30) to forty (40) percent of the variance from the mean beach function. This function, termed the "terrace function", displays a significantly broader representation than does the bar-berm function. It is evident that this function relates changes at the low-tide terrace and is based on shorter time dependent variations within the surf zone. It is important to realize that even though the amount of variation accounted for by the bar-berm and terrace functions are similar, the orthogonality of the eigenfunctions indicate that the functions are unlikely to be related to the same process.

A comparison can be made of the data bases generated in this study and that used by Uda and Hashimoto [6]. The nature of both data bases is basically similar resulting in the analysis procedures being comparable. It is interesting to note that in each study the eigenfunction corresponding to the largest eigenvalue related to the mean value function. Their respective second eigenfunctions also showed a resemblance to each other indicating that similar processes were taking place. Each is associated to a relatively long time periodicity with the former function representing seasonal longshore transport about the longshore intervals and the latter relating seasonal onshore-offshore transport about an axis normal to the shoreline.

As mentioned previously, variations of principal component analysis procedures have been used successfully in numerous areas of research and not just to study changes in coastal beach profiles. A case in point is the handling of sound velocity profile (SVP) data which are used in the prediction of underwater sound propagation loss [LeBlanc and Middleton (8)]. SVP's are computed from data including temperature, salinity, etc., versus depth for a large number of locations throughout the world's oceans. Due to a large number of monitoring sites (estimated at about 40,000) and the quantity of data being supplied it became imperative to devise a method and summarize all the historical data in such a way as to reveal inner-statistical dependence between SVP data points. Each individual SVP profile is stored in the form of a sound velocity value for each of twenty-eight (28) standard ocean depths. As there is considered to be a great deal of statistical overlap within the twenty-eight point SVP matrix the dimensionality of the data set is reduced into orthonormal functions. These empirical orthonormal functions (EOF) are eigenvectors derived from the data covariance matrix. Each eigenvector is scaled by the square root of its eigenvalue so as to be weighted according to their relative significance in the fitting process. Since the SVP matrix is dimensioned from the twenty-eight standard ocean depths, the covariance matrix will yield twenty-eight eigenvalues and vectors. The authors acknowledge that three to four vectors will account for up to ninety-eight (98%) percent of the total variance. Since each eigenvector is independent it represents an individual mode of SVP behavior. In other words, this particular eigenvector can be associated with a distinct physical driving mechanism in the ocean

area. A graphical review of sample EOF's showed that the first function had its greatest departure from the mean velocity profile at the surface. This would mean that surface effects account for most of the energy in the excess sound velocity variation in this vector. A graph of this vector does not exhibit any nodes or zero crossings. A plot of the second EOF indicates a zero crossing occurring at a relatively shallow depth with the vector maintaining a broad, prominent variation at greater water depths. Subsequent vectors contained an additive increase of zero crossings while showing less and less distinctive characteristic behavior.

This research further expanded upon the use of the empirical orthonormal functions to characterize SVP space-time behavior over a large geographical area. In this procedure a mean value profile and covariance matrix for the entire ocean area data set is obtained. The variations are considered to be a function of latitude, longitude and month of year. As only four EOF's were required to accurately represent a given SVP data set this expanded procedure contructs a covariance matrix from truncated vector sets. This new truncated matrix is considered more stable since the EOF's with low signal-to-noise ratios have been removed by the reconstruction process. For each of the four components of the truncated matrix a two by seventh order Chebyschev polynomial was used by the authors to characterize the mean value over the span of latitude, longitude and month. The result of this computation yielded an entire band of mean value variation for the ocean. By defining the area and month a truncated matrix of mean value variations could be calculated. A

corresponding covariance matrix is calculated from which contributions to the original mean value profile can be made and, hence, a new mean SVP is found. The coefficients of the generated EOF's are now capable of being represented as characteristic contour maps of the ocean area. General characteristics of sound velocity profiles at specific geographical locations could now be investigated.

The use of principal component analysis for time series data can be extended to include combinations of several data sets. This capability is demonstrated by Kutzbach [9] as he investigated the combined representation of fields of three climatic variables. Specifically, the eigenvectors are derived from data readings of monthly mean sea-level pressure, surface temperature and precipitation taken at twenty-three (23) points throughout North America. The three variables selected were chosen because the inter-relations between their mean fields have been closely studied in the past making it possible to evaluate the usefulness of the combined eigenvector representations. To assure that each variable, at each point in the field, is of equal importance the variables are normalized to have zero means and unit variances. The data is arranged as a matrix of values with dimensions equal to the product of number of climatic variables and locations throughout North America by the the number of observations. The dimension of the constructed symmetric matrix is then also dependent upon the number of climatic variables desired in the analysis. The eigenvalues and corresponding eigenvectors are now calculated by standard eigen analysis techniques. In simpler terms, eigenvector patterns are derived from the twenty-five (25) fields of

observed normalized departures from the mean. Eigenvector patterns can be obtained by plotting each of the twenty-three (23) components of the eigenvectors at each of the geographic locations. To help clarify the resulting plots, isolines are drawn. Since these isolines are derived from the normalized departure fields they are nondimensional. It should be pointed out that a representation of combined patterns would not necessarily resemble the representations of individual patterns unless the variables in question are uniquely related.

A comparison of cumulative percentages for various combinations of variables shows that combined representations prove to be more efficient than separate representations. As example, six eigenfunctions derived in the combination of two climatic variables, pressure and temperature, are responsible for nearly eighty-four (84%) percent of the total variance. Individually, pressure and temperature require five and four eigenfunctions, respectively, for a total of nine functions to represent the same amount of total variance. This efficiency turns out to be a function of the correlation between the fields of variables. Generally, the number of eigenfunctions required to explain a certain variance is inversely related to the degree of correlation between the climatic variables.

The accuracy in interpreting the eigenvector patterns is dependent on several factors. First, the significance of the statistical quantities calculated is dependent on the number of observations. Second, the smallest scale of resolution depends on the

spatial density of the measuring locations. Third, the distribution of explained variance between climatic variables is dependent on the weighting procedure used to normalize the variables. Finally, the departure patterns depend on the temporal density of the data obtained.

Thus far, principal component analysis has been used to describe characteristic representations involving time series data bases. The advantage of this analysis method to represent large swarms of data can also be applied to spectral data for ocean waves. Any given spectrum may contain as many as one hundred frequency bands, making it somewhat difficult to reduce to observed processes. Needless to say, the degree of difficulty drastically increases as more and more spectra are introduced.

The basic multi-dimensional nature of wave spectra lends itself well to principal component analysis. It is known that the ocean surface can be represented by an energy spectrum. When a spectrum is calculated from collected data the statistical characteristics of the process are assumed to remain statistically stationary. Eventually the total wave energy will vary causing variations in the statistical characteristics. As the spectra and associated characteristics change throughout time it is the probability distribution of these different properties that define the spectral characteristics for the ocean climate.

Vincent and Resio [10] used eigenvector analysis to analyze the

characteristic types of variation within sample spectra. Initially, a mean value vector was determined and removed from each observation leaving a deviation matrix. A covariance matrix is formed from the product of the deviate matrix and its transpose. The eigenfunctions are then derived based on this covariance matrix. The eigenvectors, termed characteristic spectral functions (CSF), are representative of the basic modes or characteristic variations in spectral shape through time. The authors obtained wave spectra from three independent sites located on the Great Lakes with a total of over 3,000 spectra available. After the CSF were calculated it was found that the first function at each site accounted for approximately sixty (60%) percent of the total variance. The combination of the first two CSF improved this representation to between seventy (70%) and eighty (80%) percent. The range of total percent variance for the first ten functions ranges from ninety-two (92%) to ninety-seven (97%) percent. The result of this finding is of fundamental interest in that many frequency components of a spectrum may be replaced by as few as ten CSF's with only a three to eight percent loss of information.

A closer look at the CSF's show that the first function closely resembles the mean value spectrum in shape. The peak of the mean spectrum corresponds approximately to the peak of this function. This first eigenfunction is found to represent a storm process since it is weighted lightly, or even negatively, during calm seas. During stormy seas it is weighted with large positive values. The second CSF provides additional variation to the mean by shifting energy to the higher frequencies when weighted positively. When weighted negatively

the energy of the spectrum is taken from the higher frequencies and moved into the lower frequency range. The form of subsequent CSF's increase in complexity and exhibit multiple peaks. The third and fourth CSF's show little consistency among the three sites studied. This inconsistency and the fact that the remaining CSF represent very little of the total variance lead to the conclusion that these are necessary only to maintain the balances between power density and the equilibrium range of the spectrum and the growth of individual storms.

In summary, principal component analysis is shown to be an important method in providing a simplified representation of time-sequence or spectral data. It also has the ability to characterize major components of variations or values of the data base since the eigenfunctions are independent and fitted to maximize the explained variance. Most importantly, vast swarms of time-series data or spectra may be reduced to only a few functions while still maintaining the inherent statistical characteristics of the original data base. The ability to reduce swarms of data is readily apparent as illustrated in Table 2. This summary reviews the number of functions required to accurately reconstruct the original data bases utilized in the studies outlined.

Table 2. Number of eigenfunctions required to reconstruct the original data base.

Research Study	Field of study	Nature of data base	Number of functions	Total percent variance
[5]	Longshore beach profile changes	Time-sequence	3	75
[6]	Longshore beach profile changes w/a breakwater	Time-sequence	*	*
[7]	Beach profile changes normal to the shoreline	Time-sequence	4	96
[8]	Underwater acoustic sound velocity profiles	Time-sequence	3	95
[9]	Combine three climatic meteorological variables	Time-sequence	10	85
[10]	Wave spectra for the Great Lakes	Spectral	10	92 - 97

* information not supplied

CHAPTER III

MATHEMATICAL DEVELOPMENT

Derivation of the eigenfunctions

It is known that movement of the sea surface can be represented by a power spectrum of a random process. This wave spectrum represents the spectral properties of the sea for a given time frame and as the wave energy varies so will the statistical properties of each spectrum. It is then the probability distribution of these different spectral properties that define the spectral characteristics of the wave climate.

In this formulation for the compact representation of a swarm of wave spectra, the notation $G(f)$ will be used to signify a single-sided power spectral density at the frequency f. Further, $G(f_j)$ will be considered a single, discrete representation ranging over the frequencies associated with short-period gravity waves. A wave spectrum can also be represented as a vector $\underset{\sim}{G}(f_j)$ consisting of N values of power density corresponding to N frequency bands. Theoretically, the wave climate could consist of an infinite number of wave spectra but for practicality the wave climate will be considered to consist of M spectra each of which is calculated for a consistent set of frequencies $f_1, f_2, \ldots f_N$. This swarm of wave spectra can also be represented mathematically in an N x M observation matrix, G_{ji}. The ith column of G represents the ith record of the swarm while

the jth row represents the temporal variation of power density in frequency f_j.

The mean power spectral density vector of the observation matrix is calculated as follows

$$\underset{\sim}{\overline{G}} = \frac{1}{M} \sum_{j=1}^{M} \underset{\sim}{G}_i \quad . \tag{1}$$

To detrend the observation matrix the mean vector is subtracted from each observation resulting in a deviation, or deviate matrix given by

$$\underset{\sim}{D}_i = \underset{\sim}{G}_i - \underset{\sim}{\overline{G}} \quad . \tag{2}$$

An associated covariance matrix is now calculated by the product of the deviate matrix and its transpose. This covariance matrix,

$$C = \frac{1}{M} DD^T \tag{3}$$

is an N x N matrix where c_{ji} is the covariance between power density in frequency band f_j and power density in frequency band f_i. The trace can be found by the summation of diagonal elements within the covariance matrix

$$\text{Tr } [C] = \sum_{j=1}^{N} C_{jj} \quad . \tag{4}$$

Utilizing the covariance matrix, an orthogonal transformation is defined by the eigenproblem

$$C\Phi = E\Phi \tag{5}$$

where E is an N x N diagonal matrix of eigenvalues e_1, e_2, ... e_N and where Φ is an N x N matrix of the corresponding eigenvectors $\underset{\sim}{\phi}_1$, $\underset{\sim}{\phi}_2$, ... $\underset{\sim}{\phi}_N$. Each eigenvector is normalized to have an Euclidean length of one. It should be noted that $e_1 \geq e_2 \geq \ldots \geq e_N$ and, in addition, each eigenvalue represents the variance in the sample explained by the associated eigenvector, $\underset{\sim}{\phi}_j$. The individual variances are found by

$$\text{variance} = \frac{e_j}{\text{Tr } [C]} \quad . \tag{6}$$

Since a linear transformation has been applied it is possible to define each original spectrum, $\underset{\sim}{G}_i$, as a linear combination of the $\underset{\sim}{\phi}$. This is illustrated by the equation

$$\underset{\sim}{G}_i = \underset{\sim}{\bar{G}} + \sum_{j=1}^{N} \underset{\sim}{\phi}_j W_{ji} \tag{7}$$

where w_{1i}, w_{2i}, ... w_{Ni} represent scalars.

The result of this process is that the organization of the sample data is now more efficiently represented in terms of the variance explained. Since the values of e_j are of a decreasing sequence, each successive value represents less and less of the total explained variance. It is therefore reasonable to expect that for some cutoff, k, the amount of variance associated with an eigenvalue, e_k, is so small that it may be suspect to computational or other errors. In

effect, the total variance of the remaining eigenvalues is so minimal that deletion of this variance is found to be unimportant in the reconstruction of the observations. Based upon this determination, the original problem can now be simplified in terms of the number of parameters required. This simplification is given as

$$\hat{\underset{\sim}{G}}_i = \underset{\sim}{\bar{G}} + \sum_{j=1}^{k-1} \underset{\sim}{\phi}_j W_{ji} \qquad (8)$$

where $\hat{\underset{\sim}{G}}_i$ represents the reconstructed observation matrix. This expression, in actuality, provides only a close approximation to the original data set since a slight portion of the total variance has now been neglected.

Computation of ship responses

Ship responses for both pitch and heave are determined based upon the design wave spectrum chosen and a given set of RAO's. Letting N represent the number of frequency bands, f_j, for which the wave height spectrum and the RAO's are determined the pitch response of the ship is given by

$$P(f_j) = Y_\phi(f_j)G(f_j) \quad . \qquad (9)$$

The corresponding heave response is found by the equation

$$H(f_j) = Y_z(f_j)G(f_j) \quad . \qquad (10)$$

For each case, the ship RAO's are excited by the original sea

observation matrix resulting in independent pitch and heave reponse matrices. By using the procedure for deriving eigenfunctions outlined previously these matrices are able to be analyzed based on their own empirical eigenvalues and associated eigenvectors.

Computation of spectral moments and spectral characteristics

Spectral moments are used to characterize a spectral distribution. The general form for the nth spectral moment is

$$m_n = \int_0^\infty f^n \, G(f) \, df \quad . \tag{11}$$

The following characteristics are then derived from the spectral moment values:

significant wave height

$$H_s = 4.0 \, (m_0)^{\frac{1}{2}} \quad ; \tag{12}$$

root-mean-square wave height

$$H_{rms} = 2.0 \, (m_0)^{\frac{1}{2}} \quad ; \tag{13}$$

spectral broadness

$$\epsilon = \left[1 - \frac{m_2^2}{m_0 m_4} \right]^{\frac{1}{2}} \quad ; \tag{14}$$

crest period

$$T_c = \left[\frac{m_2}{m_4} \right]^{\frac{1}{2}} \quad ; \tag{15}$$

and, zero crossing period

$$T_z = \left[\frac{m_0}{m_2} \right]^{\frac{1}{2}} . \qquad (16)$$

CHAPTER IV

COMPUTATIONAL PROCEDURES

Analysis of problem formulation

All analyses and computations for this research study were conducted using a computer program written specifically for this research. The program consists of a main section, fifteen subroutines and three function subroutines. Due to the sensitivity of portions of this analysis, all calculations, where applicable, were conducted using double precision. In essence, this program consists of six primary groupings. The major group contains all calculations and functions necessary to perform the eigen analysis routine on either wave or response spectra. Three other groups evaluated spectral values in regards to their statistics and moments for each of the wave, pitch and heave response spectra, respectively. The fifth primary group allowed for selection of a set of ship RAO's and for the computation of pitch and heave response values when excited by the given wave spectra. These five groupings comprise the functional portion of the program. A flow chart of these groupings is illustrated in Appendix I. The sixth and final primary group consists of the presentation of the input data, test values, statistics and various other general output. The format of the program output format is listed in Appendix II.

Sea spectra

Testing for ship response characteristics was conducted using three basic groups of wave spectra to excite the ship/model response amplitude operators over a specified continuous range of frequencies. The first group consisted of the standard spectral models Pierson-Moskowitz, JONSWAP and Ochi-Hubble. Generally speaking, Pierson-Moskowitz represents a relatively smooth spectral shape and a moderate peak. JONSWAP, on the other hand, is noted as a sharp, narrow-peaked spectrum which will contain a marked increase in wave energy from the Pierson-Moskowitz spectrum for the same parameters. Spectral density values for both of these spectral models can be derived using only a single parameter, usually wind speed or significant wave height. The third model is the Ochi-Hubble spectrum [11] which is more complex than the previous two as the power density values are derived only after specifying six independent parameters. The total spectrum is then expressed by the combination of two sets of three-parameter spectra. The formulations for the considered "most probable spectrum" was used in this research work. This derived spectrum is relatively wide band and exhibits multiple peaks. Formula for these three models are outlined in Appendix III.

The fourth wave spectrum used in testing was derived from actual time series wave height data obtained at Shell Oil Company's Cognac Platform [12]. This raw data was transformed into its spectral form by the Blackman-Tukey method for the frequencies desired. Therefore, the eight separate records of wave data provided were able to be converted into eight individual spectra. Finally, an additional

spectrum was synthetically generated by the superposition of two independent spectra thereby resulting in a new, wider spectrum with a very distinct second peak. The purpose for analyzing ship responses excited by this spectrum is to investigate the capability of the eigen analysis to reconstruct the ship response caused by spectra of unique or extreme shapes.

Response amplitude operators (RAO's)

Three sets of ship RAO's were selected for use in calculating vessel response. The ship response spectra were obtained by exciting the RAO's with a given wave spectrum. Although ships and marine vessels have six degrees of freedom, or motion, only two were investigated in this study. These two were pitch and heave motions. Each set of RAO's had been determined through model tests in a towing tank, then scaled to represent the tested ship. The first two ship RAO's were for a "series 60" basic model and scaled to a 500 foot long ship [13]. Model specifics are detailed in Appendix IV. The first RAO represented the ship travelling at a speed of 12 knots in high irregular seas. The second set of series 60 operators were also for a speed of 12 knots but for moderate irregular seas. The third and final set of RAO's [14] were also obtained from model tests but were scaled to a 350 foot long U. S. Coast Guard Cutter. The response operator curves were generated by the superposition of model responses to regular waves. The equivalent test ship speed was 10 knots.

CHAPTER V

NUMERICAL EXAMPLES

Sea spectra

The first phase of this research study examined the statistical properties of various data sets in their original and compacted forms. The data sets analyzed include spectra derived from three spectral models, spectra obtained from the superposition of two individual spectra and a set of real wave spectra. Each original set of data was evaluated for mean statistics and standard deviations of significant wave height (H_s), root-mean-square of wave height (H_{rms}), spectral broadness, crest period, zero crossing period and spectral moments. The reconstructed spectra obtained by principal component analysis were also evaluated for their own statistics. Except for spectral broadness, each value obtained for the reconstructed spectrum either matched or fell within the bounds of deviation for the original data base. In only one-half of the cases studied did the values of spectral broadness exceed the standard deviation bounds. However, for these cases the range was exceeded by less than one-half on one percent ($< 0.5\%$). Some statistics for both the original and reconstructed spectra are presented in Table 3. It is clear that reconstructed wave spectra do statistically represent their original data set. Therefore, representation of a wave data base by its reconstructed spectrum is justified.

Table 3. Statistics of spectral wave data bases.

Test Run	Sign. Wave Height (FT)	RMS Wave Height (FT)	Spectral Broadness	Crest Period (SEC)	Zero Cross. Period (SEC)	Zeroth Spect. Moment	Second Spect. Moment	Fourth Spect. Moment (10^{-2})
1A	16.38	11.58	.723	5.46	7.98	148.96	2.05	6.59
B	5.79	4.09	.030	.71	1.39	12.35	.75	.80
C	17.26	12.21	.756	5.58	8.52	148.96	2.05	6.59
D			*0.22*					
2A	20.26	14.33	.721	5.98	8.71	228.40	2.64	7.08
B	7.26	5.36	.031	.80	1.55	155.90	.97	.79
C	21.37	15.11	.755	6.10	9.31	228.40	2.64	7.08
D			*0.42*					
3A	16.94	11.98	.760	4.89	7.54	153.96	2.61	10.92
B	4.88	3.45	.026	.02	.34	83.34	1.21	5.14
C	17.55	12.41	.772	4.88	7.69	153.96	2.61	10.92
D								
4A	12.96	9.17	.819	4.12	7.19	84.10	1.63	9.61
B	.47	.33	.007	.07	.19	6.10	.09	.58
C	12.97	9.17	.820	4.12	7.19	84.10	1.63	9.61
D								

Test run code:

1. Pierson-Moskowitz spectra
2. JONSWAP spectra
3. Ochi-Hubble spectra
4. Real data spectra

A. mean of original wave spectra
B. standard deviation of the original wave spectra
C. statistic value of the reconstructed spectrum
D. percent (%) exceeding the deviation range

The amount of total variance explained by the compaction process for six sample data sets are listed in Table 4. The high percentage values obtained provides yet another indication that the reconstructed spectra do account for most of the variation within the original data

Table 4. Selected statistics for six data bases tested.

Data Base No.	Data Base	Percent Variance of CSF1	Spectral Broadness	Zeroth Moment	Total Variance Explained	Number of Functions
(1)	Pierson-Moskowitz (P-M)	95.1	0.755	148.96	99.9	2
(2)	JONSWAP	78.1	0.755	228.40	78.8	2
(3)	Ochi-Hubble	96.6	0.772	154.00	99.9	2
(4)	Real data	83.8	0.820	84.10	99.9	2
(5)	Modified (P-M)	95.3	0.714	201.04	99.9	2
(6)	Modified JONSWAP	78.2	0.714	308.32	93.0	2

set. A look at the other values included indicates that spectral broadness and the zeroth moment (area under the spectrum) can effect the "ease" with which the total variance is explained. In comparing data bases (1) and (3) they were found to have similar values of broadness and moment. Therefore, it is significant to note that the amount of variance explained by their first characteristic spectral function was approximately the same. A comparison of data bases (1) and (2) show similar values of broadness but a relatively large difference in moment. It is found that CSF1 accounts for less

explained variance in the base with the higher of the two moment values. With this in mind it is important to understand why the amount of explained variance in data base (4) is small even though it has a small moment value and a relatively broad shape. The theoretical data sets contain M spectra all of the same spectral form and are varied only by a single parameter. This creates uniform variation of spectral characteristics thoughout the data base. The real data base also consists of M spectra but with a unique set of characteristics for each spectrum. Therefore, since there is more inherent characteristic variation within the real data base its first CSF is unable to explain as much variance when compared to the theoretical data bases.

A second approach was followed to again monitor the sensitivity of the compaction process to spectral broadness. To accomplish this, two theoretical wave spectra are combined prior to compaction as shown in Fig. 6. If taken independently, the second spectrum would represent thirty-five (35%) percent of the area under its "parent" spectrum. The parent and modified spectrum are then combined allowing a predetermined frequency shift, f, to exist between the peaks. By varying the shift in frequency the effects of spectral broadness can be detailed since the spectral energy remains constant. The statistics for each test case are listed in Table 5. For a constant Hs (Hs being proportional to the zeroth moment), the percent of variance explained by CSF1 increases as the spectra broaden. This reaffirms the previous conclusion that, generally speaking, for two wave spectra with the same energy, the one that is broadest will be

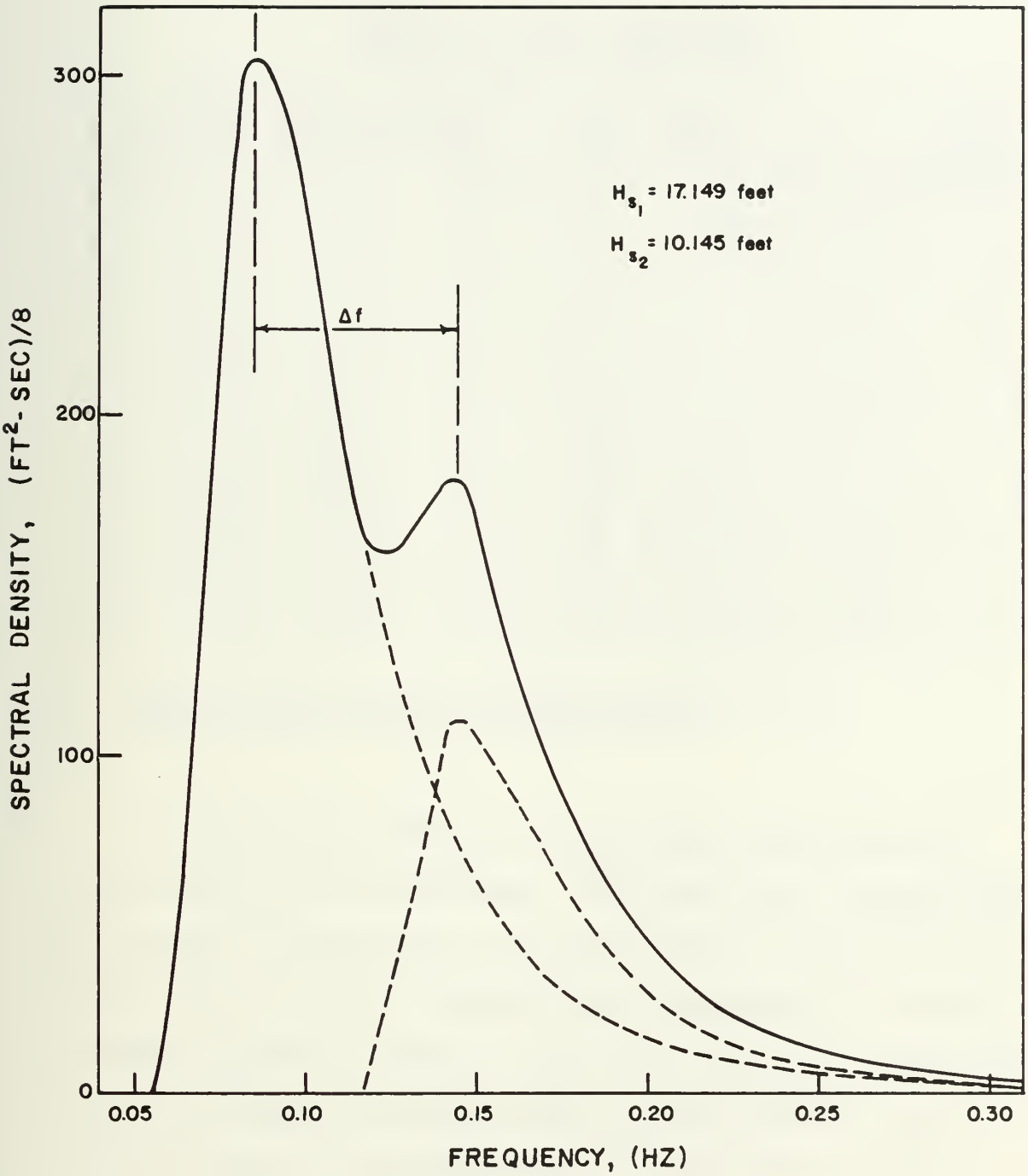

Fig. 6. Two Pierson-Moskowitz spectra superimposed with a 0.06 hertz frequency shift.

the easiest to reconstruct.

Table 5. Selected statistics for the wave data bases tested.

Test Run	Phase Shift (f)	Percent Variance of CSF1	Spectral Broad-ness	Sign. Period (SEC)	Sign. Wave Ht. (FT)	Total Variance	Number of CSF Required
5	0.02	96.36	.738	5.51	20.05	101.63	2
5	0.04	96.43	.724	5.38	20.05	101.56	2
5	0.06	95.71	.716	5.20	20.05	104.79	2
5	0.08	95.36	.714	4.97	20.05	107.39	2
6	0.02	83.29	.736	6.02	24.83	99.45	2
6	0.04	78.63	.721	5.85	24.83	81.71	2
6	0.06	78.15	.714	5.61	24.83	92.58	2
6	0.08	78.19	.714	5.32	24.83	93.05	2

5. Pierson-Moskowitz spectra modified by superposition
6. JONSWAP spectra modified by superposition

As the shape and statistics of wave spectra change the ship response spectra will also change. For the test cases just mentioned, the response characteristics were also obtained for pitch and heave. These values are listed in Tables 6 and 7, respectively. A review of the heave statistics in Table 7 reveals that they closely follow the same trends evident in the wave spectra values, Table 5. This is expected, however, since the amplitude of heave motion is closely related to the amplitude of the exciting wave. It is also significant to note that for each test case, the percent of variance explained by the heave CSF1 very closely approximates the corresponding value of

Table 6. Selected statistics for pitch response using two modified wave data bases and RAO set 1.

Test Run	Phase Shift (f)	Percent Variance of CSF1	Spectral Broad-ness	Sign. Period (SEC)	Sign. Pitch Motion (DEG)	Total Variance	Number of CSF Required
5	0.02	97.37	.323	8.26	9.88	97.37	1
5	0.04	98.98	.315	8.10	9.96	98.98	1
5	0.06	97.73	.333	7.94	9.43	97.73	1
5	0.08	94.51	.364	8.00	8.57	99.43	2
6	0.02	82.30	.338	8.49	11.91	98.92	4
6	0.04	73.74	.323	8.23	12.31	97.84	3
6	0.06	79.48	.349	7.97	11.63	97.24	3
6	0.08	64.21	.399	8.04	10.25	97.88	4

Table 7. Selected statistics for heave response using two modified wave data bases and RAO set 1.

Test Runt	Phase Shift (f)	Percent Variance of CSF1	Spectral Broad-ness	Sign. Period (SEC)	Sign. Heave Motion (FT)	Total Variance	Number of CSF Required
5	0.02	96.18	.440	8.79	17.66	99.81	2
5	0.04	96.42	.449	8.52	17.28	99.71	2
5	0.06	95.54	.474	8.33	16.68	99.65	2
5	0.08	95.00	.496	8.39	16.00	99.64	2
6	0.02	83.19	.433	9.20	22.47	98.86	3
6	0.04	79.15	.449	8.81	22.07	98.55	3
6	0.06	78.79	.484	8.50	21.34	98.53	3
6	0.08	78.73	.513	8.56	20.35	98.45	3

the wave CSF1. Therefore, the resulting shape and statistics of a ship's response spectrum is highly dependent on the shape and statistics of the wave spectrum used to excite the ship. For the pitch statistics it is found that no general trend is readily apparent nor are there any definite similarities with the wave spectrum statistics. This is a good indication that the ship motions in pitch are strongly dependent on the given ship's characteristics and the way in which they interact with the wave spectrum.

Pitch and heave response spectra

The second phase of this research study involved using both original and compact data sets to compute ship responses and characteristics. As with the wave spectra, statistics were generated for the M original response spectra and the reconstructed response spectrum. In addition, statistics were calculated for the response spectrum generated by the compact wave spectrum exciting the ship RAO's. The statistics for the reconstructed response spectrum matched extremely well with the statistics of the response spectrum obtained from the compact wave spectrum. These statistical values, except for spectral broadness of the heave spectra, were within the original range of standard deviation. In only one-quarter of the cases studied did the values of spectral broadness for heave spectra exceed the standard deviation bounds. In these cases the range was exceeded by less than six percent ($< 6\%$) of the original value.

The effect that spectral broadness and zeroth moment have on the

ability to accurately reconstruct original response bases was also determined. For two theoretical response spectra, with the same broadness, the one with the higher value of moment will be the most difficult to reconstruct. Conversely, for two theoretical spectra with the same value for zeroth moment, the one that is narrower will prove to be the most difficult to reproduce accurately.

It is understood that the product of a wave spectrum and a ship RAO yields the response spectrum. It is also known that the ship RAO is a "characteristic" of that ship and can only be changed by a physical modification to the ship or its contents. Therefore, the wave spectrum is the "influence" causing the characteristic response amplitude operators to yield the response spectrum. Further analysis was conducted in regards to the reconstructed response spectrum CSF to find any physical correlation between the RAO's and response spectrum. Since the amount of variance explained by the first CSF (CSF1) is large, any effects by the higher functions would be negligable and are disregarded.

Figures (7) and (8) graphically show a set of ship RAO's with their associated CSF1 and response spectrum. In these graphs the pitch and heave CSF1's closely resemble the original wave spectrum. It can be seen how a wave spectrum the shape of CSF1 would combine with the ship RAO to achieve the response spectrum. Figure (9) illustrates a similar graph but for an Ochi-Hubble spectrum. Both the response spectrum and CSF1 exhibit a distinctive second peak, however, a second peak is not readily apparent on the original wave spectrum.

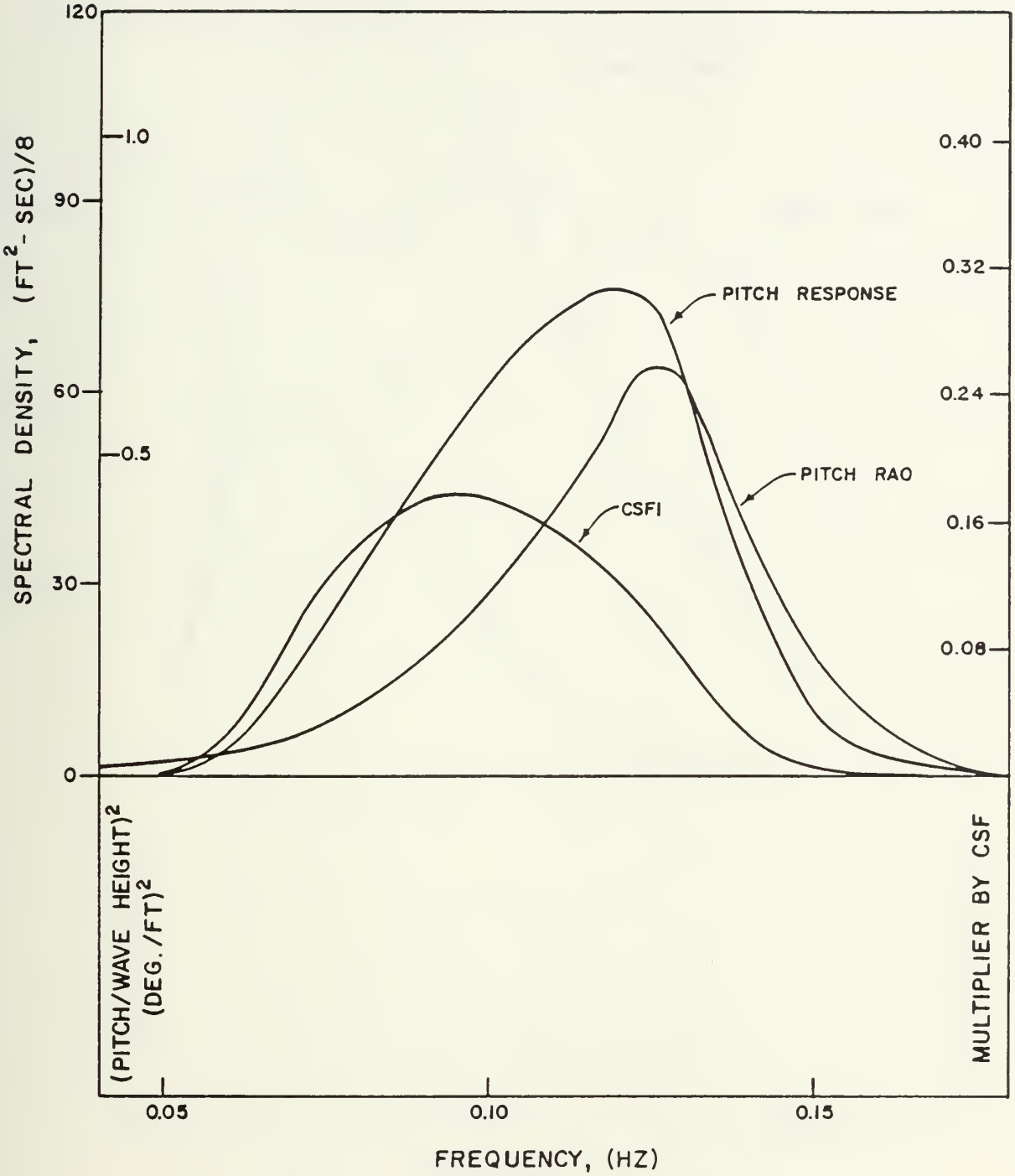

Fig. 7. Ship pitch response, pitch CSF1 and pitch operator (RAO set 1) using the Pierson-Moskowitz wave data base.

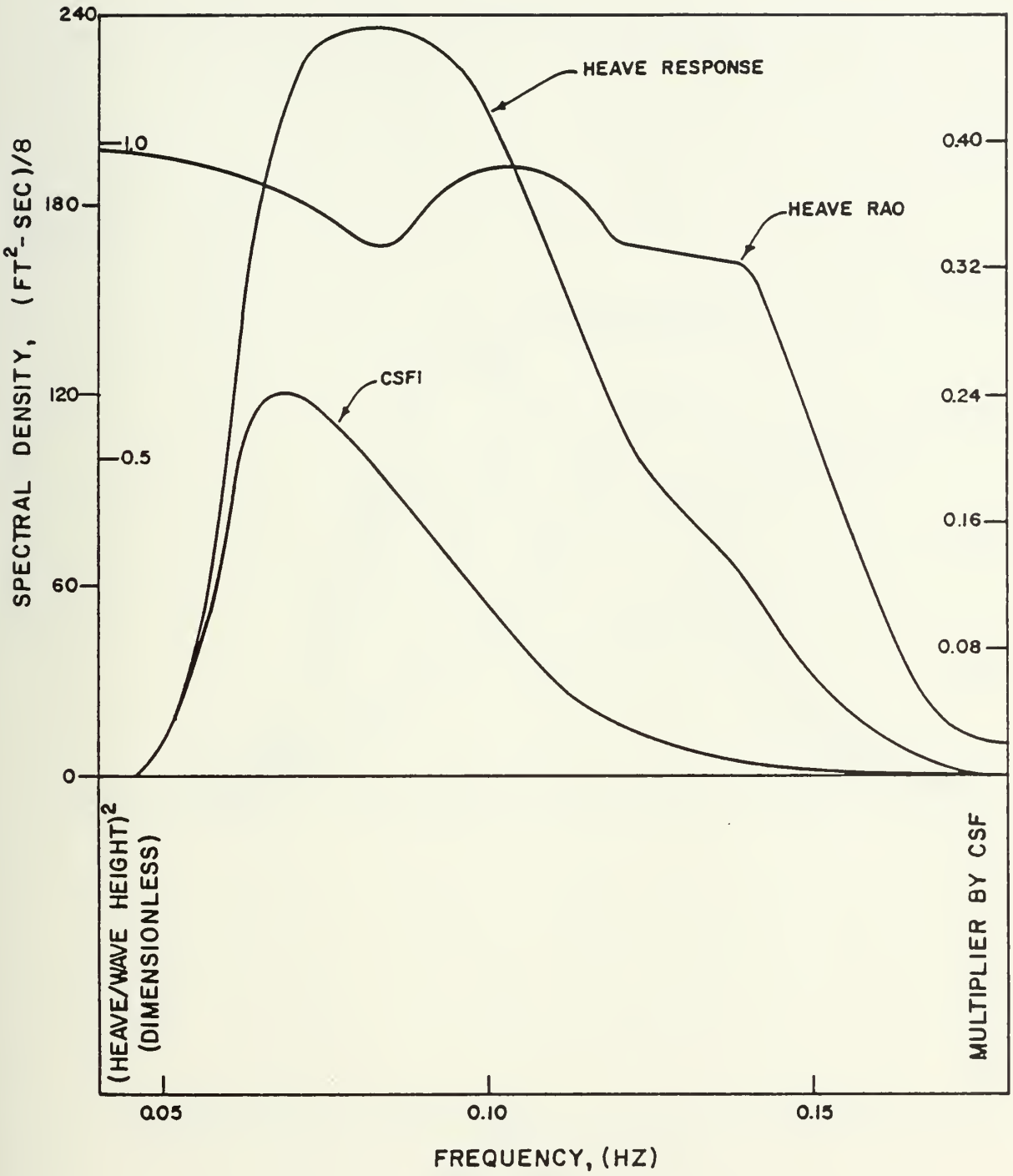

Fig. 8. Ship heave response, heave CSF1 and heave operator (RAO set 1) using the Pierson-Moskowitz wave data base.

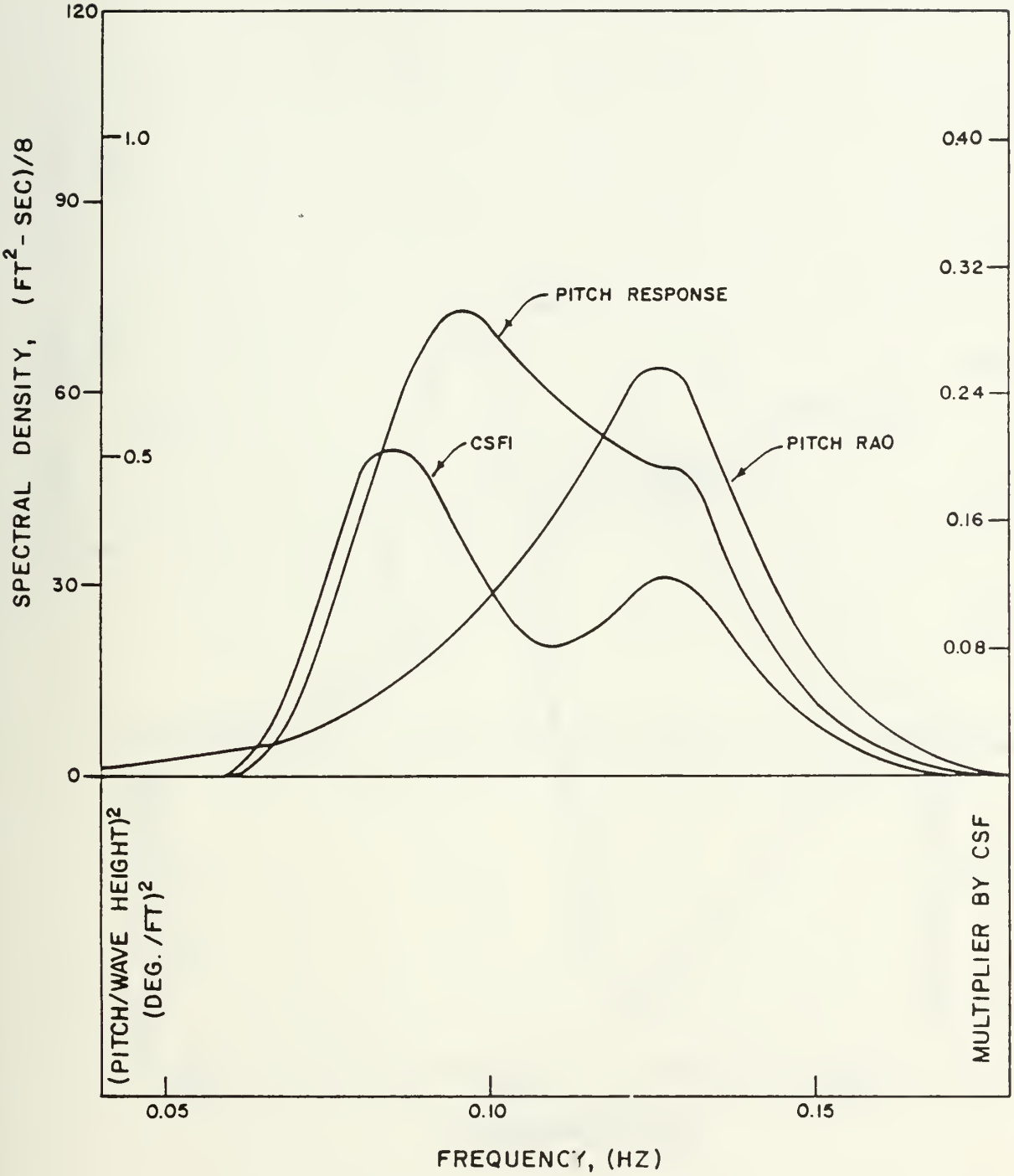

Fig. 9. Ship pitch response, pitch CSF1 and pitch operator (RAO set 1) using the Ochi-Hubble wave data base.

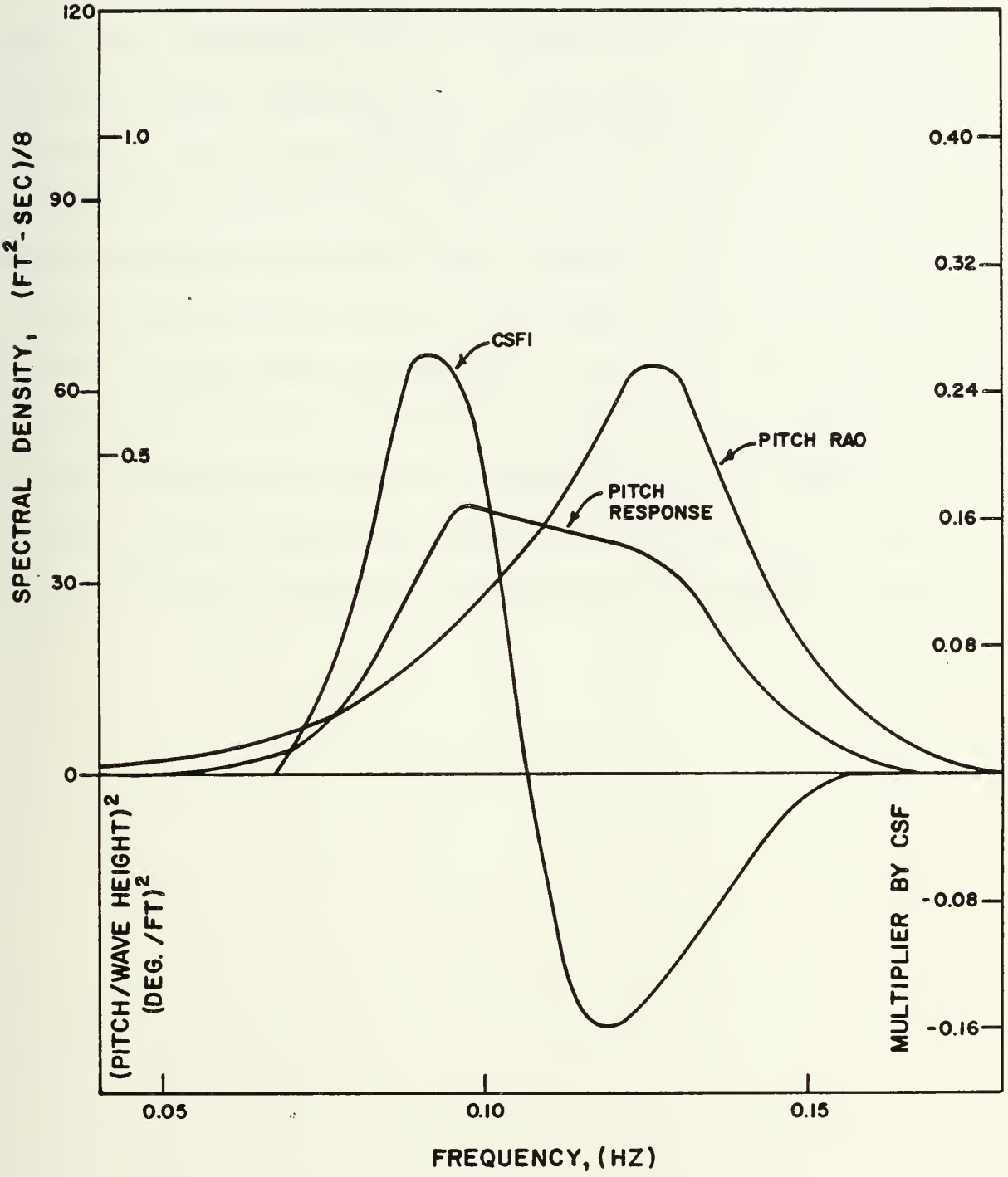

Fig. 10. Ship pitch response, pitch CSF1 and pitch operator (RAO set 1) using the real wave data base.

Graphically it is shown how the characteristic ship RAO is either amplified or restricted by CSF1. A similar effect is experienced with the heave response spectrum but by a lesser degree. The wave spectrum for the real data is a relatively smooth form with no multiple peaks or other unique distinctions. A plot of the pitch response spectrum and corresponding CSF1 in figure (10) indicates negative CSF values within a short frequency range. It is evident that within this range the pitch response levels off and begins a negative slope. The overall effect, is one of negating the positive RAO peak. Based on the investigations conducted it is apparent that since the RAO function does not change, CSF1 represents the effect or "influence" the exciting wave spectrum has in producing the corresponding response spectrum.

CHAPTER VI

SUMMARY AND CONCLUSIONS

In the first phase of research it was found that the statistical properties of the various wave data bases studied could be accurately represented by their compacted forms. This held true for both synthetic and real wave data sets.

The second phase noted that ship response spectra could be equally well represented by a compact spectrum. The statistics for the reconstructed spectra were also found to be well within numerical bounds.

The results of this study lead to the following conclusions:

1. Principal component analysis is capable of compacting data bases representing wide ranges of spectral form into usable representable spectra for ship design.

2. The statistics of reconstructed spectrum compare extremely well with statistics of the original data base for the synthetic and real data examined in this study.

3. In general, the more narrow-banded or higher in energy the spectrum is, the more difficult it becomes to reconstruct.

4. The statistics of the ship response spectrum, using a compacted

wave spectrum to excite the ship RAO's, compares favorably to the statistics of the original response spectra.

REFERENCES

1. Comstock, J.P., editor, Principles of Naval Architecture, Society of Naval Architects and Marine Engineers, New York, 1967.

2. St. Denis, M. & Pierson, W.J., "Motions of Ships in Confused Seas," SNAME Trans., Vol. 61, 1953, pp. 280-357.

3. Michel, W.H., "Sea Spectra Simplified," Marine Technology, Jan. 1968, pp. 17-30.

4. Niedzwecki, J.M., "Compact Spectral Representation of Surface Wave Data," Engineering Mechanics in Civil Engineering, Vol. 1, 1984, pp. 728-730.

5. Hashimoto, H. and Uda, T., "Field Investigation of Beach Profile Changes and the Analysis Using Empirical Eigenfunctions," Coastal Engineering, 1982, pp. 1369-1384.

6. Uda, T. and Hashimoto, H., "Description of Beach Changes Using an Empirical Predictive Model of Beach Profile Changes," Coastal Engineering, 1982, pp. 1405-1418.

7. Winant, C.D., Inman, D.L. and Nordstrom, C.E., "Description of Seasonal Beach Changes Using Empirical Eigenfunctions," J. of Geophysical Research, Vol. 80, No. 15, 1975, pp. 1979-1986.

8. LeBlanc, L.R. and Middleton, F.H., "An Underwater Acoustic Sound Velocity Data Model," J. Acoust. Soc. of Am., Vol. 67, No. 6, Jun. 1980, pp. 2055-2062.

9. Kutzbach, J.E., "Empirical Eigenvectors of Sea-Level Pressure, Surface Temperature and Precipitation Complexes over North America," J. of Applied Meteorology, Vol. 6, Oct. 1967, pp. 791-802.

10. Vincent, C.L. and Resio, D.T., "An Eigenfunction Parameterization of a Time Sequence of Wave Spectra," Coastal Engineering, 1977, pp. 185-205.

11. Ochi, M.K. & Hubble, E.N., "Six-Parameter Wave Spectra," Coastal Engineering, 1976, pp. 301-328.

12. Obtained from F.W. Boye, Manager, Production Operations, Research Department, Shell Development Company, Houston, Tx.

13. Lewis, E.V., "Ship Speeds in Irregular Seas," SNAME Trans., Vol. 63, 1955, pp. 134-223.

14. Obtained from Dr. Roger Compton, Naval Architecture Department, United States Naval Academy, Annapolis, Maryland, 14 January 1985.

APPENDIX I

COMPUTER PROGRAM FLOW CHART

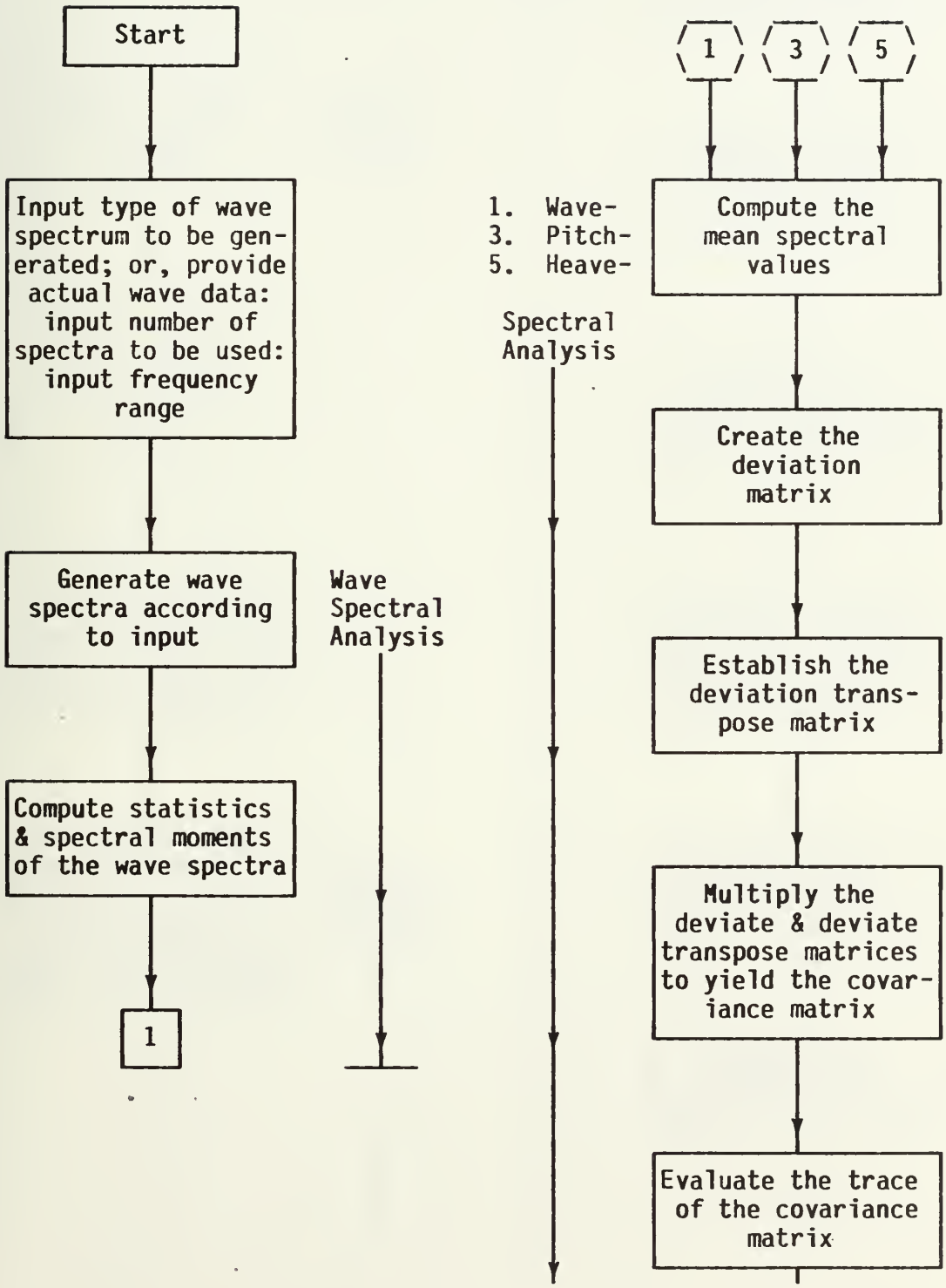

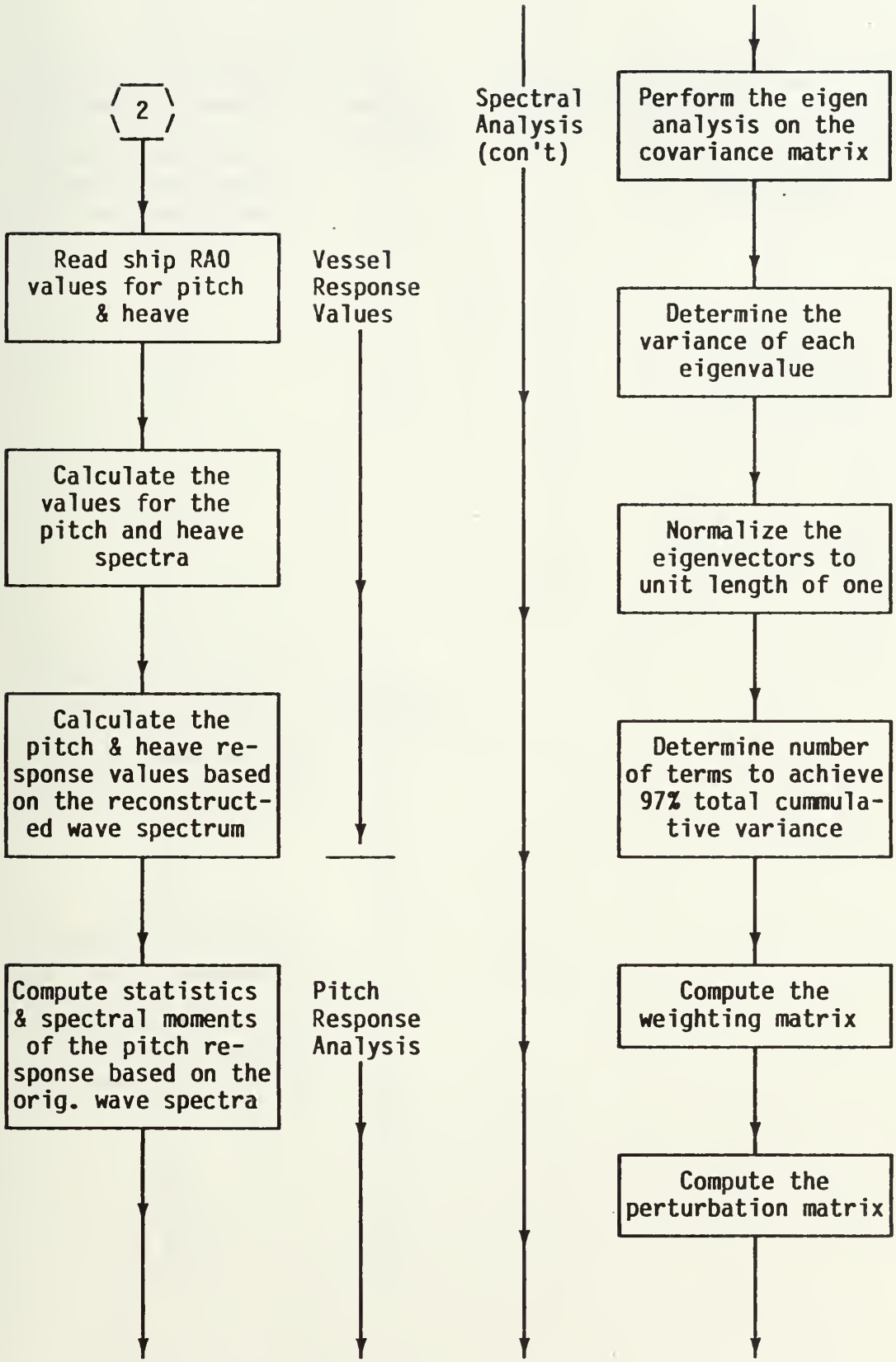
2
Read ship RAO values for pitch & heave
Calculate the values for the pitch and heave spectra
Calculate the pitch & heave response values based on the reconstructed wave spectrum
Compute statistics & spectral moments of the pitch response based on the orig. wave spectra
Vessel Response Values
Pitch Response Analysis
Spectral Analysis (con't)
Perform the eigen analysis on the covariance matrix
Determine the variance of each eigenvalue
Normalize the eigenvectors to unit length of one
Determine number of terms to achieve 97% total cummulative variance
Compute the weighting matrix
Compute the perturbation matrix

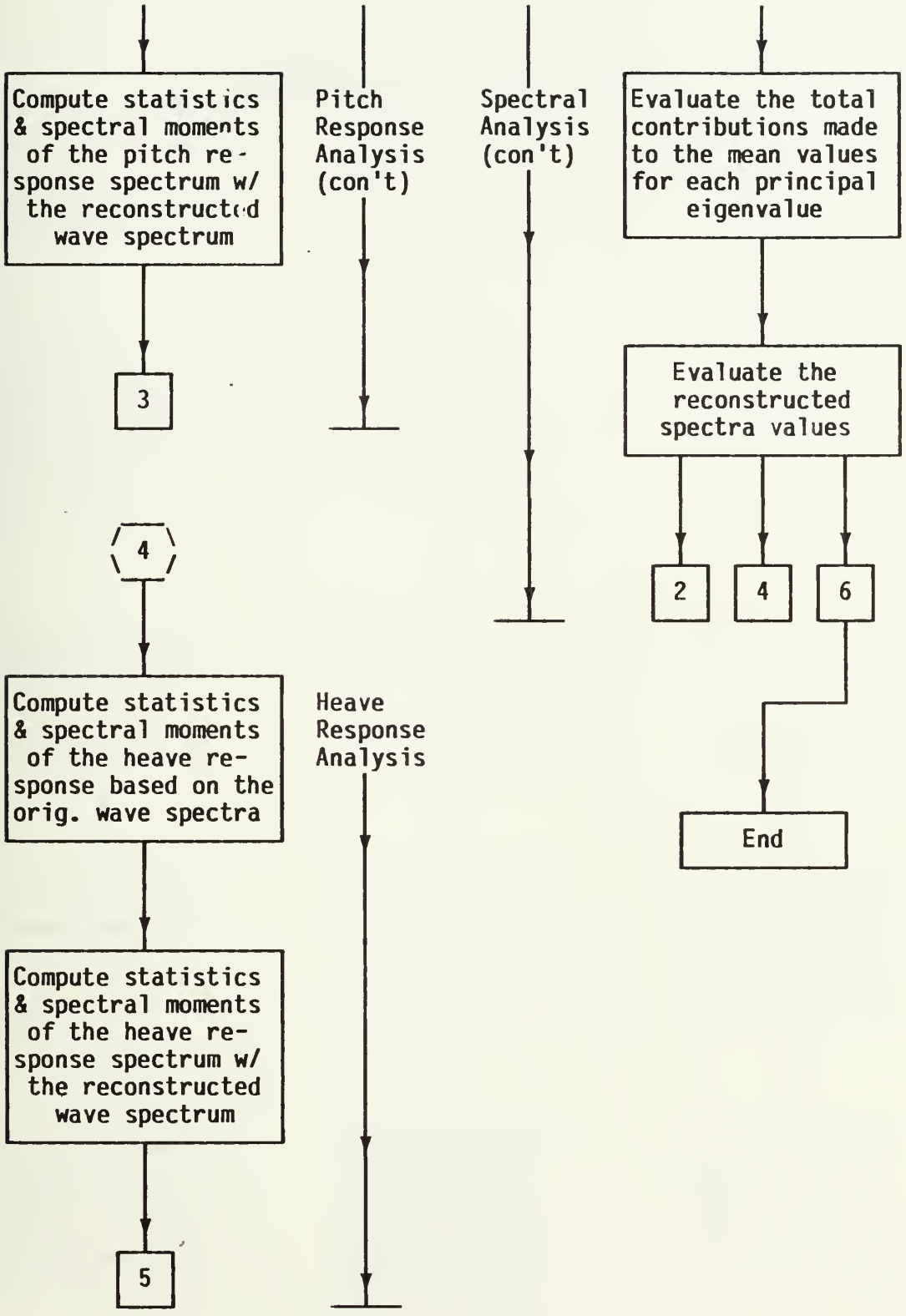
Compute statistics & spectral moments of the pitch response spectrum w/ the reconstructed wave spectrum
3
Pitch Response Analysis (con't)
Spectral Analysis (con't)
Evaluate the total contributions made to the mean values for each principal eigenvalue
Evaluate the reconstructed spectra values
2
4
6
End
4
Compute statistics & spectral moments of the heave response based on the orig. wave spectra
Heave Response Analysis
Compute statistics & spectral moments of the heave response spectrum w/ the reconstructed wave spectrum
5

APPENDIX II

COMPUTER PROGRAM OUTPUT FORMAT

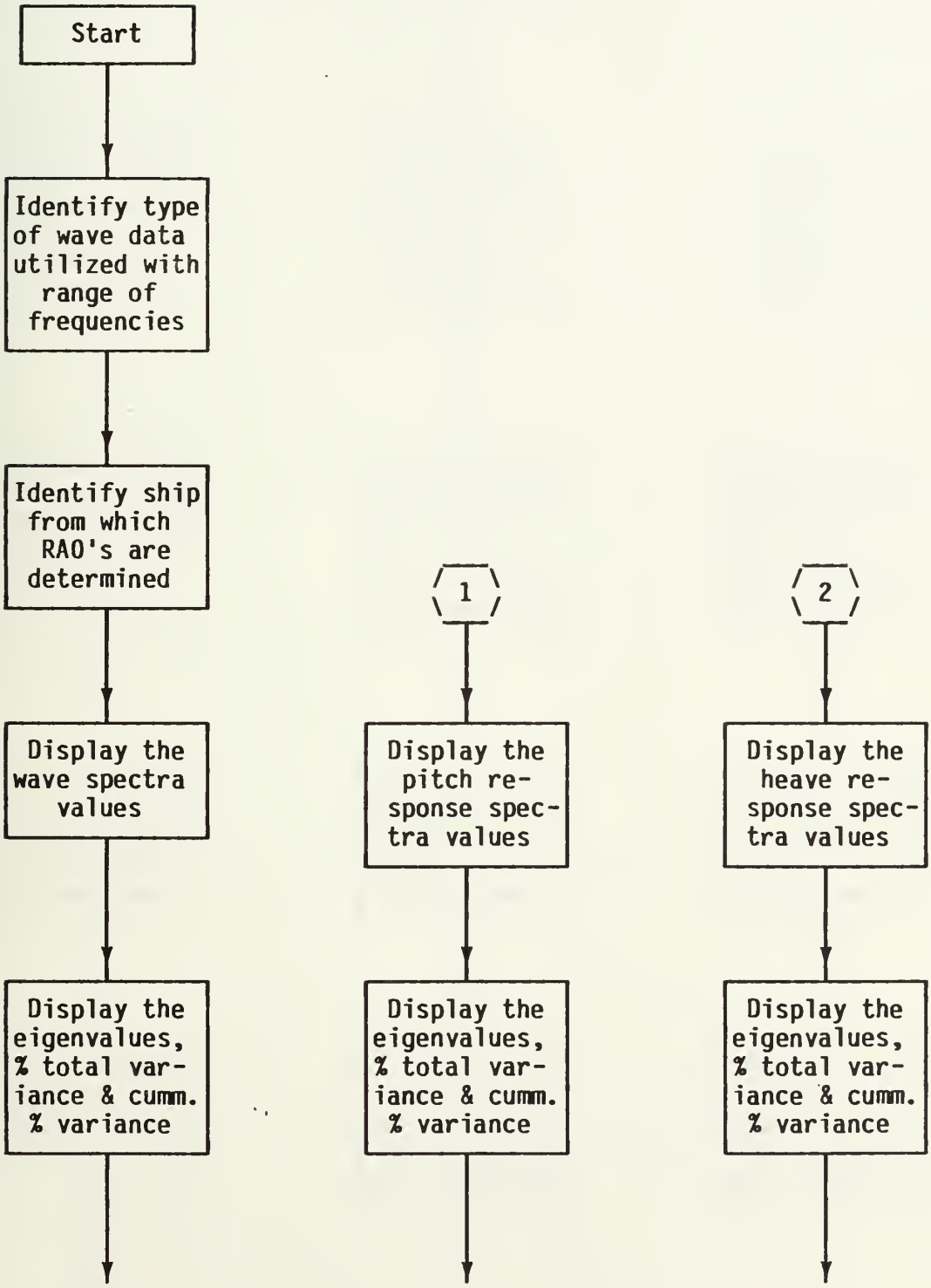

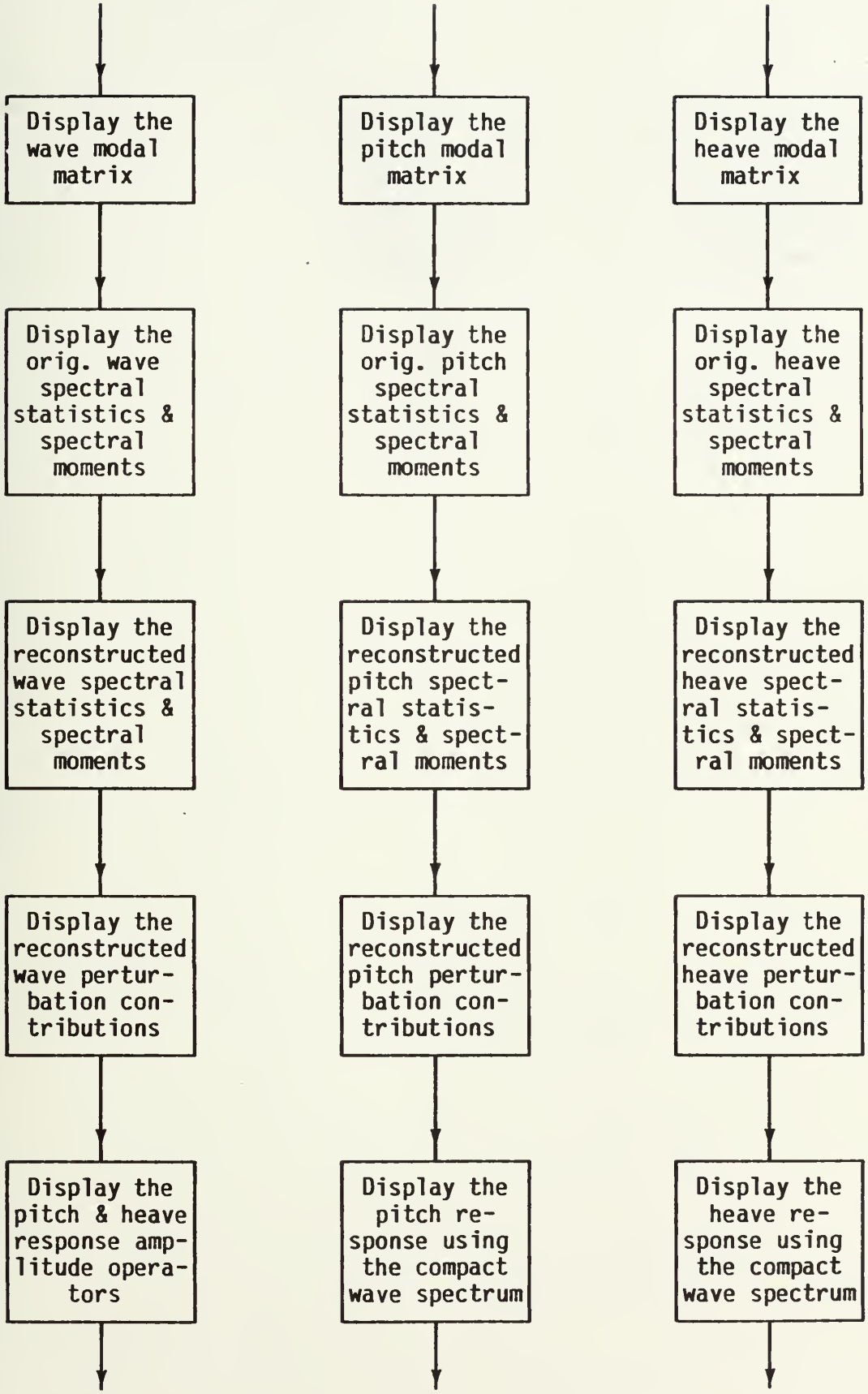
Display the wave modal matrix
Display the pitch modal matrix
Display the heave modal matrix
Display the orig. wave spectral statistics & spectral moments
Display the orig. pitch spectral statistics & spectral moments
Display the orig. heave spectral statistics & spectral moments
Display the reconstructed wave spectral statistics & spectral moments
Display the reconstructed pitch spectral statistics & spectral moments
Display the reconstructed heave spectral statistics & spectral moments
Display the reconstructed wave perturbation contributions
Display the reconstructed pitch perturbation contributions
Display the reconstructed heave perturbation contributions
Display the pitch & heave response amplitude operators
Display the pitch response using the compact wave spectrum
Display the heave response using the compact wave spectrum

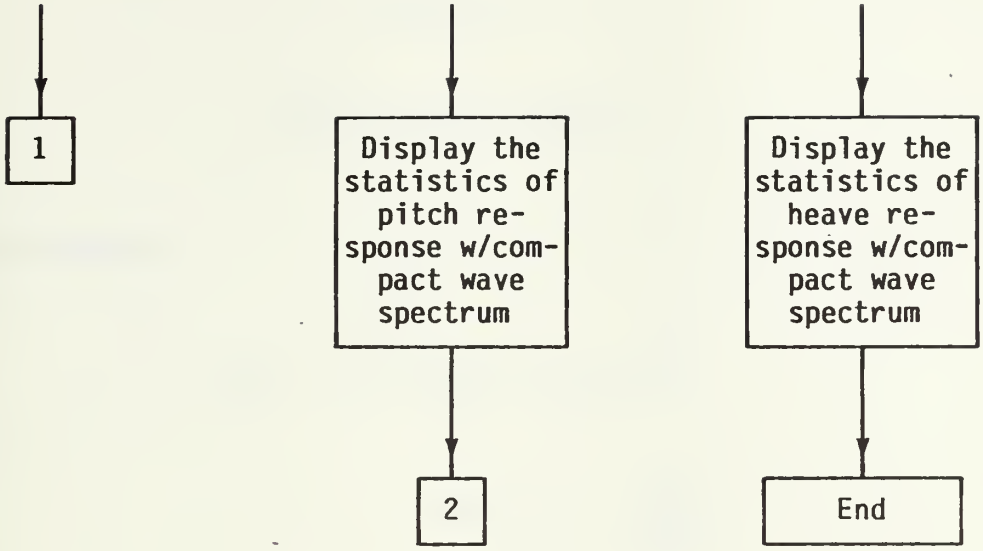
1
Display the statistics of pitch response w/compact wave spectrum
Display the statistics of heave response w/compact wave spectrum
2
End

APPENDIX III

WAVE SPECTRUM MODELS

PIERSON-MOSKOWITZ

$$\underline{G}(f) = Af^{-5}\exp\left[-0.74(f_m/f)^4\right]$$

$$\text{where,} \quad A = \frac{\alpha g^2}{(2\pi)^4}$$

$$f_m = \frac{g}{2\pi U}$$

$\alpha = 0.0081$

U = wind velocity (fps)

g = gravity

JONSWAP

$$\underline{G}(f) = Af^{-5}\exp\left[-0.74(f_m/f)^4\right]\delta^a$$

$$\text{where,} \quad A = \frac{\alpha g^2}{(2\pi)^4}$$

$$f_m = \left[\frac{0.74}{1.25}\right]^{\frac{1}{4}} \frac{g}{2\pi U}$$

$$a = \exp\left[\frac{-(f-f_m)^2}{2\sigma^2 f_m^2}\right]$$

$\alpha = 0.0081$

$\delta = 3.3$

$\sigma = \sigma_a = 0.07 \quad f < f_m$

$\sigma = \sigma_b = 0.09 \quad f > f_m$

U = wind velocity (fps)

g = gravity

OCHI-HUBBLE

$$G(f,H_s) = \frac{2\pi}{4} \sum_{j=1}^{2} A_j \bar{\Omega}^{Cj} \exp\left[-B_j \bar{\Omega}^{4}\right]$$

where, $\Omega = 2\pi f$

$C_j = (4L_j + 1)$

$B_j = C_j \Omega_{mj}^4 / 4$

$A_j = (B_j)^{Lj} H_j^2 / \Gamma(L_j)$

$H_1 = 0.84H_s$

$H_2 = 0.54H_s$

$\Omega_{m1} = 0.70\exp[-0.014H_s]$

$\Omega_{m2} = 1.15\exp[-0.012H_s]$

$L_1 = 3.0$

$L_2 = 1.54\exp[-0.019H_s]$

$$\Gamma(x) = \int_0^\infty t^{x-1} \exp[-t]\, dt$$

with x the argument of Γ.

APPENDIX IV

SHIP/MODEL CHARACTERISTICS

RAO Sets 1 & 2

Type	Series 60	
ETT Model No.	1445	
Length BP, L, (FT)	5.000	
Breadth, (FT)	0.667	
Draft, (FT)	0.267	(even keel)
Displacement (FW,LBS)	33.27	
Wetted Surface Area (FT^2)	4.27	
Block Coefficient	0.600	
Waterplane Coefficient	0.706	
Scale Factor	100.0	
Ship Length, (FT)	500.0	

RAO Set 3

Length BP, L, (FT)	5.50
Breadth, (FT)	0.66
Draft, (FT)	0.21
Displacement (FW,LBS)	23.01
Wetted Surface Area (FT^2)	3.90
Block Coefficient	0.479
Waterplane Coefficient	0.75
Scale Factor	63.6364
Ship Length, (FT)	350.0

APPENDIX V

TABLE OF NOMENCLATURE

C	covariance matrix
CSF	characteristic spectral function
CSF1	CSF corresponding to the first or largest eigenvalue
c_{ji}	element in C positioned in the jth row and the ith column
D	deviate matrix
D^T	deviate transpose matrix
E	N x N diagonal matrix of eigenvalues
EOF	empirical orthonormal function
e_j	the jth eigenvalue of E
G	N x M observation matrix
$G(f)$	single-sided power spectral density at frequency f
$\underset{\sim}{G}(f)$	vector representation of a wave spectrum
$\underset{\sim}{\overline{G}}$	mean power spectral density vector of the observation matrix
$\underset{\sim}{\hat{G}}_i$	reconstructed observation matrix
g	acceleration due to gravity
H	wave height from crest to trough
H_s	significant wave height
H_{rms}	root-mean-square wave height
$H(f_j)$	ship heave response at frequency f_j
h	component wave height
k	cutoff point at which e_k, e_{k+1} ..., e_N are neglected
M	number of spectra represented in the spectral wave data base

m_n nth spectral moment

N number of frequency bands within a wave spectrum or spectral wave data base

$P(f_j)$ ship pitch response at frequency f_j

RAO response amplitude operator

SVP sound velocity profile

T_c crest period

T_r trace of the argument matrix

T_z zero crossing period

W N x M weighting matrix

w_{ji} element in W located in the jth row and ith column

$Y_z(f_j)$ ship heave RAO value at frequency f_j

$Y_\phi(f_j)$ ship pitch RAO value at frequency f_j

z vertical distance of ship heave from origin

ϵ spectral broadness

f frequency, cycles per unit time

Φ N x N matrix of eigenvectors

$\underset{\sim}{\phi}_j$ the jth eigenvector of Φ

ρ mass density of sea water

ϕ angle of pitch

VITA

Name: Larry Donald Linn

Education:

High School Graduate (June 1975), North Thurston High School, Lacey, Washington

B.S. of Naval Architecture (May 1979), United States Naval Academy, Annapolis, Md.

Professional:

Commissioned an Ensign, United States Navy (May 1979)

Engineer-in-Training Certification, State of Pa., (July 1979)

Civil Engineer Corps Officer School, Construction Management Course (September 1979)

Assistant Resident Officer in Charge of Construction, Long Beach Naval Shipyard and Long Beach Naval Station (September 1979 - June 1981)

OSHA Safety Education Training School (February 1980)

Assigned to Naval Mobile Construction Battalion THREE for fleet construction support overseas. Duties included: Battalion Engineering Officer; Battalion Asst. Operations Officer; Bravo Co. Commander in charge of Camp Maintenance & utilities construction; Charlie Co. Commander in charge of all vertical construction; Officer-in-Charge of all construction while independently deployed to Greece (June 1981-December 1983)

Management, Leadership, Education & Training (MLET) School (February 1982)

Present:

Active duty military, Lieutenant, Civil Engineers Corps, United States Navy, assigned to post-graduate school Texas A&M University

Address:

7048 Puget Beach Rd. NE
Olympia, Washington 98506

214406

Thesis
L6636 Linn
c.1 Ship response using
a compact wave spec-
trum model.